Sustainable Cities and Society 145 (2026) 107488

Contents lists available at ScienceDirect

Sustainable Cities and Society

journal homepage: www.elsevier.com/locate/scs

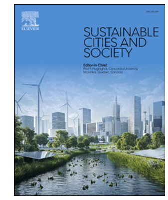

Scenario-based simulation of greening adaptation strategies in a dense historic urban fabric: a comparative analysis for the case of Naples, Italy

Francesco Sommese *, Lorenzo Diana

Department of Civil, Building and Environmental Engineering (DICEA) University of Naples Federico II, P.le Vincenzo Tecchio, 80, 80125, Naples, Italy

A R T I C L E I N F O

Keywords:
Urban Heat Island
Climate adaptation
Cooling effects
Green roof
Historical urban fabric
Microclimatic simulation

A B S T R A C T

Urban overcrowding and heat-absorbent materials, combined with a lack of greenery, create a harsh microclimate in older city centers. In the case of Naples (Italy), these critical issues are further exacerbated by the effects of climate change, which increases the frequency and duration of heatwaves, thereby heightening the vulnerability of the urban fabric and negatively affecting residents' quality of life.

This study proposes a simulation-based evaluation of greening strategies in the Castel Capuano area (Naples, Italy) as climate adaptation solutions, with particular attention to their compatibility with historical and architectural constraints. The methodology uses ENVI-met simulations to compare three scenarios: baseline, green roofs, and an integrated greening strategy. The analysis, conducted at five control points, assesses four key parameters: Potential Air Temperature (PAT), Relative Humidity (RH), Mean Radiant Temperature (MRT), and Wind Speed (WS), as well as two human thermal comfort indices: Universal Thermal Climate Index (UTCI) and Physiological Equivalent Temperature (PET).

The results indicate that, under the simulated extreme summer conditions, green roofs alone provide marginal benefits, while the integrated greening strategies show the highest microclimatic improvements among tested scenarios, including average reductions in potential air temperature exceeding 1°C, pronounced decreases in mean radiant temperature, localized variations in airflow patterns, and significant improvements in thermal comfort indices, with UTCI decreasing by 4–6°C and PET by 8–10°C within the modelled scenarios. The integrated approach emerges as the most effective strategy for mitigating the Urban Heat Island and enhancing microclimatic comfort. Moreover, it has the potential to enhance overall urban livability by making public spaces more usable, safer, and more conducive to social interaction. Such multifunctional and site-specific solutions can serve as replicable and context-specific models for other historic centers with similar morphological and climatic characteristics.

1. Introduction

The acceleration of global warming and uncontrolled urban expansion have intensified the Urban Heat Island (UHI) effect, threatening urban resilience and undermining public health and environmental stability (Chen et al., 2025; Li et al., 2025; Romanello et al., 2023). Indeed, the UHI represents one of the main environmental challenges in densely populated areas, manifesting as a consistent increase in temperatures compared to the surrounding peri-urban and rural zones. This phenomenon primarily results from anthropogenic transformations of the land surface and the ability of urban structures to absorb, store, and release heat during nighttime hours (Firozjaei et al., 2026). Although UHI is now widespread globally, its intensity is particularly pronounced in compact, high-density historic centers typical of Mediterranean cities (Salvati et al., 2019). In contexts such as the ancient center of Naples (Italy), which is representative of many comparable contexts, the intricate urban morphology, the high height-to-width ratio of streets, the use of low-reflectance construction materials, and the scarcity of green spaces combine to generate unfavorable local microclimates, amplify thermal discomfort, and exacerbate adverse effects on public health (Cafaro et al., 2024; Fortelli et al., 2016). Global climate change, characterized by an increase in the frequency and intensity of heat waves, further exacerbates the impact of UHI, heightening risks to human health, reducing thermal comfort, and challenging the environmental and energy sustainability of urban systems (Chapman et al., 2017). Anthropogenic alterations of the urban landscape disrupt the energy

* Corresponding author.
E-mail address: francesco.sommese@unina.it (F. Sommese).

https://doi.org/10.1016/j.scs.2026.107488
Received 7 November 2025; Received in revised form 25 February 2026; Accepted 6 May 2026
Available online 7 May 2026

balance and the distribution of solar radiation, promoting heat accumulation and reducing natural ventilation. Taken together, these factors make urban areas and historic centers especially vulnerable to the effects of global warming and the resulting health and social emergencies (Diana et al., 2024).

Among the strategies proposed to address these challenges, Nature-based Solutions (NbS) play an increasingly significant role as climate adaptation measures. By leveraging ecosystem functions and biodiversity, NbS provide cooling-related ecosystem services through multiple physical mechanisms including shading, evapotranspiration, increased soil permeability and surface albedo, and improved thermal properties of urban materials, to counter the impacts of climate change and enhance urban resilience (IUCN, 2025; Cohen-Shacham et al., 2016; Frantzeskaki, 2019; Lopez et al., 2020; Sommese & Diana, 2022)—while also delivering multiple environmental and social co-benefits, including biodiversity restoration and landscape enhancement (Sommese, 2024).

Interventions such as green roofs, vegetated façades, parks, and tree-planted courtyards have been shown to reduce surface temperatures and heat accumulation, thereby contributing to improved air quality, stormwater management, and greater usability of public spaces.

Despite their recognized potential, the large-scale adoption and integration of NbS in dense urban environments remain limited in many regions and, in some cases, largely theoretical. This limitation is particularly evident in compact historic centers, where severe constraints related to space availability, urban morphology, and heritage preservation significantly restrict the feasibility of ground-based greening strategies.

Within these constrained contexts, green roofs have emerged as one of the most practicable and widely accepted NbS, as they allow the introduction of vegetation without competing for scarce ground-level space and can often be retrofitted onto existing buildings with relatively fewer spatial conflicts.

Nevertheless, important knowledge gaps persist regarding the combined effectiveness and spatial distribution of multiple greening interventions implemented simultaneously in high-density historic centers.

This research gap is particularly evident for historic and architecturally valuable contexts. Most existing studies focus on single interventions in suburban areas or more recently developed districts, while analyses evaluating multiple integrated scenarios in heterogeneous historic fabrics, characterized by variable geometries, diverse construction materials, and limited permeable soil, are scarce (Diana et al., 2024; Sommese et al., 2025; Sommese & Diana, 2022, 2025).

This gap is further compounded by challenges in performance assessment, as many current building and urban climate modelling tools are primarily designed to evaluate isolated, building-scale solutions (e.g., green roofs), while their capacity to simulate interacting NbS at the neighborhood scale, particularly in historic urban contexts, is still limited. Another limitation concerns the lack of systematic investigations that integrate key microclimatic variables, such as potential air temperature, mean radiant temperature, wind speed, and relative humidity, measured and compared at multiple representative points within the urban study area. The absence of distributed measurements limits the ability to calibrate and validate numerical models, hindering a full understanding of local-scale energy exchange processes.

This study addresses these gaps by investigating the Castel Capuano area in Naples (Italy), an emblematic example of a compact, high-density historic center characterized by extremely limited green surfaces and a high susceptibility to heat accumulation. Using microclimatic simulations performed with ENVI-met on the hottest day of 2024, three scenarios are analyzed and compared: (i) a baseline scenario representing current conditions; (ii) a scenario introducing green roofs on flat coverings; and (iii) an integrated scenario combining green roofs with greening of the main courtyard, a parking area, and other surrounding spaces. The assessment, conducted at five representative points, evaluates key microclimatic parameters to provide insights into the effectiveness, feasibility, and limitations of integrated urban climate adaptation strategies for Mediterranean historic centers under increasing climate stress.

1.1. Scientific literature review

The international scientific literature on greening intervention strategies is extensive and well established, yet it remains highly differentiated according to case studies and the specific types of interventions examined. However, scenarios that integrate greening measures at both the urban and building scales are rarely explored, highlighting a gap in multiscale strategies applicable to dense, heritage-protected urban contexts. Many studies, while highlighting significant benefits, tend to focus on single solutions limited to green roofs, green façades, or isolated urban greening actions, without considering integrated approaches.

In particular, research on green roofs at the building scale provides valuable insights and promising results, but, in most cases, it assesses only the effects of the green roof as the sole "green" infrastructure, overlooking the potential synergies with other types of interventions at the urban scale, which is crucial for historic and compact urban fabrics.

Table 1 provides a concise summary of the main findings from the international scientific literature on greening strategies in the built environment, specifying for each case the reference city, the area of intervention (urban and/or building scale), and the key results or guiding principles achieved.

While many studies focus on residential or campus environments, subtropical, tropical, or cold climates, their findings may not directly apply to dense, heritage-protected Mediterranean districts such as the area of Castel Capuano (Naples, Italy) under investigation in this manuscript. Existing results are context-specific and may not be transferable to historic Mediterranean city centers, where morphology, climate, and conservation constraints differ. For example, studies in New York (Alizadehtazi et al., 2024; Smalls-Mantey & Montalto, 2021), Hong Kong (Ng et al., 2012), Melbourne (Jamei et al., 2023), and Singapore (Donthu et al., 2024) provide important insights on UHI mitigation and thermal comfort. Similarly, research from Berlin (Knaus and Haase, 2020), Xi'an (Ma et al., 2025), and New Belgrade (Kosanović et al., 2025) illustrates the effectiveness of integrated greening interventions on microclimate and thermal comfort, yet the scale, climate, and urban context differ substantially from historic Mediterranean city centers.

Zheng et al. (2021) investigated extensive green roofs in a subtropical monsoon climate: in summer these roofs provided a maximum nighttime cooling of 1.63°C but a daytime warming of up to 2.89°C, with the intensity of the effect varying according to depth.

Jahangir et al. (2024) analyzed the impact of green roof coverage on the UHI, showing that increased vegetation lowers temperatures and reduces the extent of overheated areas, with stronger effects in zones initially lacking greenery.

Other studies, by contrast, focus on residential neighborhoods but continue to examine only isolated interventions, typically limited either to green roofs or to specific greening solutions applied solely at the urban scale. For example, Knaus et al. (Knaus & Haase, 2020) evaluated green roofs in a residential neighborhood of Berlin, showing that on hot summer days they can reduce the Physiologically Equivalent Temperature (PET) by about 9 K, providing superior thermal comfort compared to street areas and mitigating neighborhood-scale heat stress. Gherri (2024, 2023) analyzed dense and compact cities and highlighted the role of urban green spaces in reducing overheating and improving thermal comfort, also considering future climate scenarios. These studies are relevant for understanding potential benefits in dense urban fabrics but still primarily focus on general urban greening rather than integrated multiscale interventions under heritage constraints.

Brahimi et al. (2023) and Tousi et al. (2025) provided examples from Mediterranean and semi-arid contexts (Athens and Djelfa respectively)

Table 1
Literature review resume. Climate[44]: Cfa- Humid subtropical; Cfb -Oceanic mild; Csa -Mediterranean hot; Cwa – Monsoon humid; BSk – Cold steppe; Af – Tropical rainforest.

Ref.	Year	City, Country	Climate	Main investigated feature	Tools/ Software	Building-scale intervention	Urban-scale intervention	Context of intervention	Demonstrated Advantages
(Smalls-Mantey & Montalto, 2021)	2021	New York, USA	Cfa	Air temperature	Field measurement	X (extensive green roof)		Modern city	−1.8°C air temperature; −18.4°C surface temperature; −0.9°C average summer nighttime temperature
(Ng et al., 2012)	2012	Hong Kong, China	Cfa	Air temperature	ENVI-met, Field measurement	X (green roof)		Modern city	To lower pedestrian-level air temperature by about 1°C, a tree canopy covering roughly 33% of the urban area is required.
(Alizadehtazi et al., 2024)	2024	New York, USA	Cfa	Air temperature	ENVI-met	X (green roof)		Modern city	−0.75 K; −0.65 K (after 4 years); −0.64 K after 7 years)
(Jamei et al., 2023)	2023	Melbourne, Australia	Cfb	Air temperature	ENVI-met, Field measurement	X (green roof)		Central area	−1.5°C air temperature; 2.38°C improvement in summer pedestrian comfort
(Zheng et al., 2021)	2021	Nanjing, China	Cfa	Air Temperature	Field measurement	X (extensive green roof)		Municipal district	−1.63°C summer nighttime; +2.89°C summer daytime.
(Jahangir et al., 2024)	2024	Tehran, Iran	BSk	Air temperature	Field measurement	X (green roof)		Municipal district	Lower temperatures
(Donthu et al., 2024)	2024	Singapore	Af	Air temperature; UTCI	Field measurement		X (cool coatings on streets)	Industrial area	−2.0°C air temperature; −1.5°C UTCI
(Knaus & Haase, 2020)	2020	Berlin, Germany	Cfb	PET	ENVI-met		X (green roofs at neighborhood scale)	Residential area	−9 K PET in summer
(Gherri, 2024, 2023)	2023	Parma, Italy	Cfa	Various	ENVI-met		X (green spaces)	Dense, compact cities	Thermal comfort, ecological, social, heat aspects
(Brahimi et al., 2023)	2023	Djelfa, Algeria	BSk	Air temperature	ENVI-met		X (green areas)	Central district	−4.75°C maximum daytime temperature
(Nourian et al., 2025)	2025	Tehran, Iran	BSk	Air temperature	ENVI-met		X (vegetation, albedo materials, green roofs)	Urban district	−1.0°C air temperature in peak summer hours
(Tousi et al., 2025)	2025	Athens, Greece	Csa	PET	ENVI-met		X (planting trees and water features)	Urban district	−14.0°C in PET
(Kosanović et al., 2025)	2025	New Belgrade, Serbia	Cfa	Outdoor thermal comfort	ENVI-met		X (effect of urban morphology)	Heritage buildings	The enhancements of green infrastructure are the only action to improve outdoor comfort
(Ma et al., 2025)	2025	Xi, China	Cwa	Outdoor Thermal comfort	ENVI-met		X (comfort of elevated open spaces)	Modern city	Optimal range for elevated green spaces (3.6–4.3 m)
(Grace et al., 2025)	2025	Perth, Australia	Csa	Surface temperatures, Air temperature	Field measurement		X (urban parks)	City	–10–15°C surface temperatures in parks.
(Yan et al., 2025)	2025	Luoyang, China	Cwa	Air temperature, PET, wind flow	ENVI-met		X (urban parks)	City	−12.3°C PET in park compared to adjacent zones
(Xiong et al., 2025)	2025	Beijing, China	Dwa	Air quality	ENVI-met		X (urban parks)	City	Improvement of air quality, microclimate, effectiveness of ENVIMET for simulation
(Zajacz et al., 2025)	2025	Budapest, Hungary	Cfb	Urban microclimate	ENVI-met, Field measurement		X (urban parks including cemeteries and hospital gardens)	City	Significant cooling and enhanced comfort
(Liu et al., 2025)	2025	Guilin, China	Cfa	UTCI, humidity	ENVI-met, Field measurement		X (investigation of canopy diameters and streets aspect ratio)	City	Reducing street aspect ratio from 1.5 to 0.9 lowers temperature and UTCI while increasing humidity; expanding canopy from 7 to 11 m produces the opposite effect.

(*continued on next page*)

Table 1 (*continued*)

Ref.	Year	City, Country	Climate	Main investigated feature	Tools/ Software	Building-scale intervention	Urban-scale intervention	Context of intervention	Demonstrated Advantages
(Leonardi et al., 2025)	2025	Catania, Italy	Csa	Air quality, thermal comfort	ENVI-met, Field measurement		X (greening strategies, innovative materials, reduction in car-traffic)	University Campus	–11.5% PM2.5; –5.9% PM10; –2.16°C UTCI for 50% traffic reduction; greening and material interventions provides complementary support.
(Qin & Zhou, 2025)	2025	Wuhan, China	Cfa	PET	ENVI-met, Field measurement		X (vegetation addition)	University courtyards	In winter: increasing PET from 9.24°C to 15.42°C (+67%); In summer: only +1.94%
(Chatterjee et al., 2019)	2019	Kolkata, India	Aw	Air temperature	ENVI-met	X (cool roofs)	X (vegetations, reflective pavements)	Neighborhood scale	−1.1°C air temperature (vegetation is more effective than cool roofs and reflective pavements)
(Heshmat Mohajer et al., 2022)	2022	Sydney, Australia	Cfa	Peak air temperature	ENVI-met	X (high albedo material)	X (urban greenery and high albedo materials)	City scale	Lowering peak temperatures by up to 1.18°C and locally by up to 4.1°C; large areas still remain warm
(Yang et al., 2025)	2025	Jinan, China	Cwa	Microclimate and air quality	ENVI-met, Field measurement	X (urban greenery)	X (urban greenery)	High-density residential areas	Shrubs reduce PM2.5 up to 65.34% more effectively than trees; Dense columnar trees lower air temperature by 3–4.8°C and PET by 8–12.8°C; Higher leaf density enhances cooling but may increase PM2.5 concentrations

showing that green spaces, trees, and water features can significantly improve thermal comfort (reductions in PET up to 14°C). These studies are more relevant for Mediterranean cities, though they typically focus on individual interventions rather than integrated multi-scale strategies.

Nourian et al. (2025) investigated the reduction of the UHI in Tehran's 12th district through the introduction of vegetation, green roofs, and high-albedo materials, demonstrating an air-temperature decrease of about 1°C during peak summer hours.

Kosanović et al. (2025) studied the Central Zone of New Belgrade to evaluate how urban morphology influences the thermal performance in a heritage-protected area, showing that target enhancements of green infrastructure remain the only practical approach to improving outdoor thermal comfort.

Other studies on urban parks, courtyards, and university campuses (Grace et al., 2025; Leonardi et al., 2025; Liu et al., 2025; Qin & Zhou, 2025; Yan et al., 2025; Zajacz et al., 2025) show the effectiveness of vegetation and water bodies in reducing temperatures and improving thermal comfort. However, the transferability of these results to dense historic districts is limited by specific climatic conditions, constrained space, and conservation requirements.

Chatterjee et al. (2019), Cuce et al. (2025), and Heshmat Mohajer et al. (2022) demonstrated the potential of integrated strategies combining vegetation with reflective materials or traffic reduction, while Yang et al. (2025) highlighted how dense residential greening can reduce air temperature and PET, emphasizing the importance of leaf density and species selection. Despite these findings, few studies explicitly address multiscale interventions in dense, heritage-protected Mediterranean city centers, underscoring the knowledge gap targeted by the present study. The integration of multiple urban greenery strategies alongside green roofs is hindered by several constraints, primarily associated with their extensive spatial requirements, as observed in landscaping interventions and large-scale green infrastructure. Such limitations, particularly pronounced in high-density urban areas, further consolidate the central role of green roofs as a robust and dependable mitigation strategy (Seidu et al., 2025). Overall, while the literature provides substantial evidence of microclimatic and thermal-comfort benefits of greening, it often overgeneralizes results from different climates and urban morphologies. Many cited benefits are context-specific, and their applicability to dense, heritage-protected Mediterranean districts remains uncertain.

1.2. Gap, aim and novelty of the research

From the existing literature, it emerges that research on greening strategies, while particularly extensive and demonstrating clear social, environmental, and sometimes economic benefits, has primarily focused on contexts that differ significantly from compact historic centers, such as the historic core of Naples or other cities with similar morphological, architectural, and climate characteristics.

Although some studies have addressed historic centers, these are generally limited to localized interventions, such as courtyards or small open spaces, which have low replicability and, crucially, do not consider combined applications of greening strategies at both the building and urban scales. For example, Naboni et al. (2023) tested mitigation strategies using vertical natural shading inspired by cacti to reduce direct solar radiation in the cloister of San Sepolcro in Parma, demonstrating improved thermal comfort while providing shading without impeding courtyard ventilation. This reveals a gap in integrated, multiscale greening strategies tailored to dense, heritage-protected urban contexts.

It should also be noted that, although scientific literature offers valuable insights on individual technologies and the effects of greenery, it does not provide a comprehensive framework for the integrated and feasible application of these strategies to a protected historic center like Naples. There is, therefore, a lack of integrated evaluation of interventions at both the building and urban scales, specifically designed for historic contexts where protected buildings and dense urban fabrics limit intervention possibilities.

Specifically, the literature reveals three main gaps:

- Studies predominantly focus on modern buildings, campuses, parks, or residential neighborhoods;
- Strategies are generally single-scale or isolated, without integrating building- and urban-scale interventions;
- There is no evidence of how greening can preserve and enhance historical and architectural heritage while simultaneously delivering microclimatic, social, and recreational benefits.

These gaps directly inform the specific objectives of the present study, which are:

- To evaluate the effectiveness of integrated greening strategies at both the building and urban scales in a dense and historic district;
- To assess, through simulation-based comparative analysis, the impact of these interventions on microclimatic parameters (air temperature, relative humidity, wind) and human thermal comfort indices (PET, UTCI);
- To propose strategies that enhance social and recreational spaces without compromising historical and architectural heritage;
- To provide replicable design guidance for similar historic urban fabrics.

The present study aims to address these gaps by proposing integrated strategies for the historic center of Naples, specifically in the Castel Capuano area, and by comparatively evaluating their microclimatic and thermal comfort performance, showing the potential of integrated greening interventions to improve outdoor microclimate environmental conditions, create new social and recreational spaces, and preserve historical and architectural value.

2. Methodology

The following section provides a detailed description of the methodology adopted in the present study, offering a step-by-step explanation of the procedures carried out and the rationale behind the choices made. These elements are presented in close connection with Fig. 1, which provides a schematic and summarized representation of the overall process.

2.1. Context analysis: area and object of study

The study area is located within a portion of the historic center of Naples, characterized by a high-density urban fabric, predominantly historic buildings with compact geometries, and numerous flat roof surfaces. This configuration makes the area particularly prone to urban heat accumulation, a typical feature of Mediterranean historic and dense centers. Castel Capuano (Fig. 2) is one of the oldest fortified buildings in Naples and stands at one end of Via dei Tribunali, the ancient main axis of the *decumano maggiore*. Located on the eastern edge of the historic center, recognized as a UNESCO World Heritage Site and among the largest in Europe, it is set within a dense and stratified urban fabric, characterized by compact historic buildings, narrow streets, and a strong concentration of residential, commercial, and cultural functions (Aveta, 2022). The area preserves the rigid street grid of Greco-Roman origin with few large open public spaces and limited green areas, factors that significantly affect the local environmental quality. Traditionally, in the historical center of Naples, green areas emerged as enclosed private courtyards, offering vital microclimatic benefits within the low-rise urban morphology (Galanti & Maria, 1872; Pane, 1971). Over the centuries, rising population density, the gradual intensification of the built environment, vertical additions and in-ward horizontal extensions, along with major alterations in spatial layouts have also brought about a

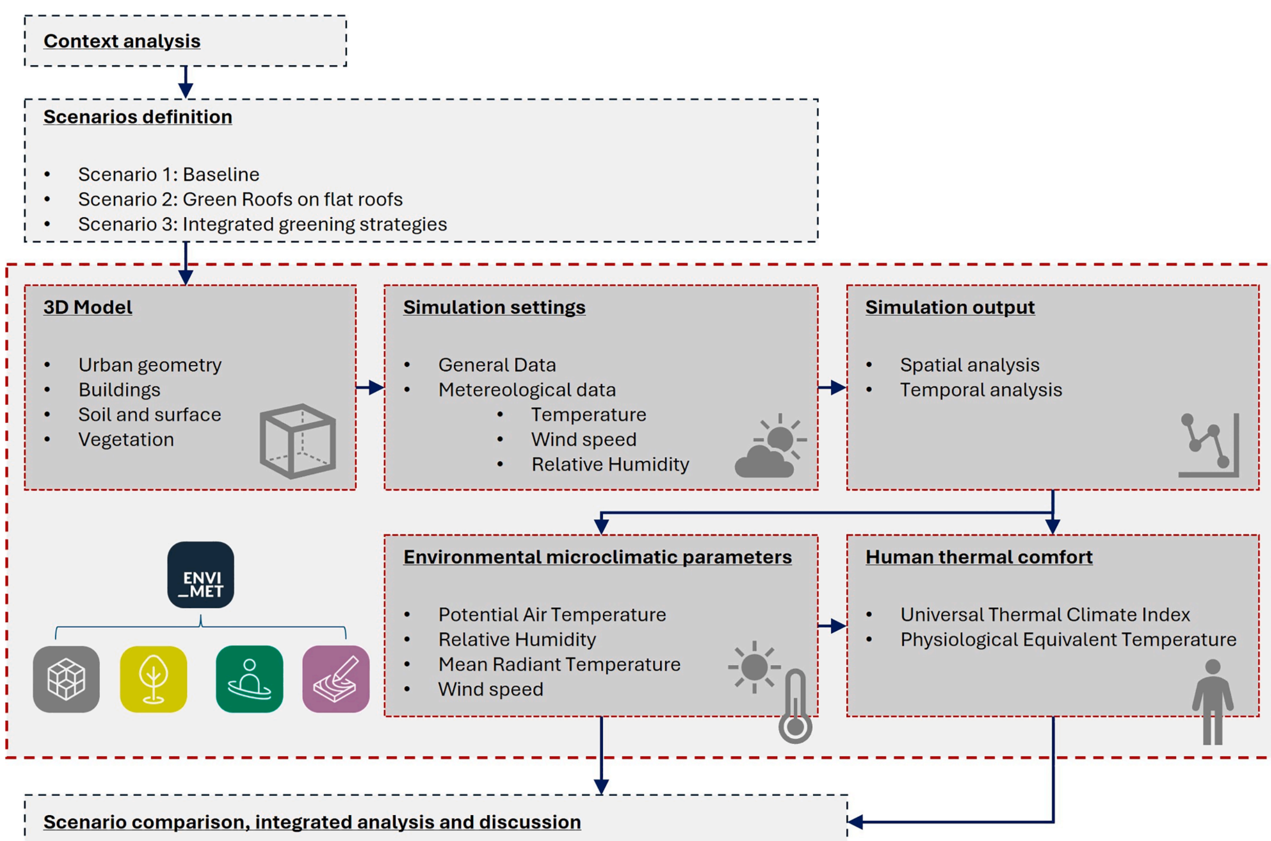

Fig. 1. Research methodological framework.

Fig. 2. Three-dimensional views of Castel Capuano. Source: GoogleMaps.

marked decline in inner private green spaces, thereby diminishing the global environmental quality and urban resilience (Sommese et al., 2025).

Despite occupying a strategic position near Porta Capuana, an historic gateway to the ancient city, and being located in an area rich in architectural heritage, the site of Castel Capuano lies within a district long neglected in terms of urban maintenance. In recent years, however, it has been the focus of restoration and enhancement projects.

Its history is a journey through the centuries. Built in the 12th century by the Normans as a royal residence, the castle underwent significant transformations under Angevin and Aragonese rule. The decisive turning point came in the 16th century, when it was converted into the seat of the city's judicial authority, earning the name "Palazzo della Vicaria".

With its six levels and up to 150-200 rooms per floor, Castel Capuano stands as an extraordinary example of architectural evolution. Beyond its imposing structure, it houses a wealth of artistic treasures and has played a crucial role in the history of the Neapolitan School of Law (Aveta, 2022). From a typological and technological point of view, in its current state, the building is organized around several courts. The largest one, looking westward, has a surface around 920 m^2. The external wings forming the building perimeter are mainly covered by sloped roofs, while internal blocks feature flat roofs. From a technological and structural point of view, the building is characterized by a thick load-bearing tuff masonry with double facing layers and rubble infill, reflecting the original fortification function. The floor slabs are of composite type, reflecting the various historical interventions and alterations over time.

2.1.1. Context analysis: climate-environmental context

From a climatic perspective, Naples has a typical Mediterranean climate (Köppen classification Csa (Arnfield, 2026)) characterized by hot and dry summers. In recent years, a marked increase in summer temperatures has been observed, with values often exceeding 35°C and, during the 2022, 2023, and 2024 seasons, exceptional peaks above 40°C for several consecutive days (Zuccaro & Leone, 2021). High relative humidity has further exacerbated thermal discomfort, making urban conditions particularly challenging for the population.

The historic center of Naples, particularly the area surrounding Castel Capuano, is highly vulnerable to heatwaves due to its compact urban morphology: narrow alleys, tall buildings, and the prevalence of impermeable surfaces limit ventilation and promote heat accumulation, intensifying the UHI effect. The near-total absence of vegetation and green spaces reduces environmental resilience, making the area less livable during the summer months and negatively affecting public health. Furthermore, the extensive sealed surfaces hinder effective stormwater management. At the same time, however, the area offers significant potential for climatic redevelopment through measures such as surface depaving, the creation of micro green areas, and the installation of green roofs compatible with architectural constraints.

Within this context, some buildings, mostly belonging to specific typologies such as courtyard houses, cultural complexes, religious institutions, or hospitals, often characterized by cloisters or large internal courtyards, stand out for their extensive surfaces. Their dimensions go beyond the scale of the single building, approaching that of large urban complexes, and play a significant role in shaping the microclimate of the surrounding fabric (Diana et al., 2024; Sommese & Diana, 2022). In such cases, the adoption of greening strategies, such as the introduction of rooftop greenery or the enhancement of internal courtyards as climatically active spaces, represents an effective measure not only to mitigate the impacts of climate change but above all to foster adaptation to these transformations, improving urban comfort and strengthening the city's environmental resilience.

2.2. Multiple scenarios definition and three-dimensional modeling

In order to identify the most effective strategies for improving microclimatic comfort and reducing temperatures, three intervention scenarios were defined (Fig. 3). These scenarios were developed on the basis of the current configuration of Castel Capuano trying to respect its historical value.

The scenarios considered are:

- Scenario 1 (S1): baseline;
- Scenario 2 (S2): green roofs on flat surfaces;
- Scenario 3 (S3): integrated greening strategies.

The definition of these scenarios makes it possible to analyze both the effectiveness of individual interventions and the mutual effect of their combination, in line with integrated approaches widely discussed in the literature for mitigating the UHI effect and supporting climate adaptation strategies in urban areas (Norton et al., 2015).

For the microclimatic modeling, ENVI-met was used, a high-resolution three-dimensional software developed to simulate interactions between urban surfaces, vegetation, and the atmosphere (Salata et al., 2017; Tsoka et al., 2018). This tool is widely adopted in urban microclimate studies for assessing the effectiveness of green solutions in high-density contexts.

The model was configured by inputting detailed data on urban geometry, surface materials, vegetation cover, and vegetative parameters. Three distinct models were then developed, each corresponding to one of the defined design scenarios (Table 2). A three-dimensional grid of 60 $\times$ 60 $\times$ 25 cells (length, width, height) was used, with each cell measuring 3 $\times$ 3 $\times$ 2 m (dx, dy, dz).

The input data for the Envimet simulations relating to the three scenarios, described in the previous paragraphs, are summarized in Table 3.

2.2.1. Scenario 1: baseline

The urban area surrounding Castel Capuano, in Naples, presents morphological and material characteristics that significantly influence the UHI phenomenon, generating critical issues in terms of

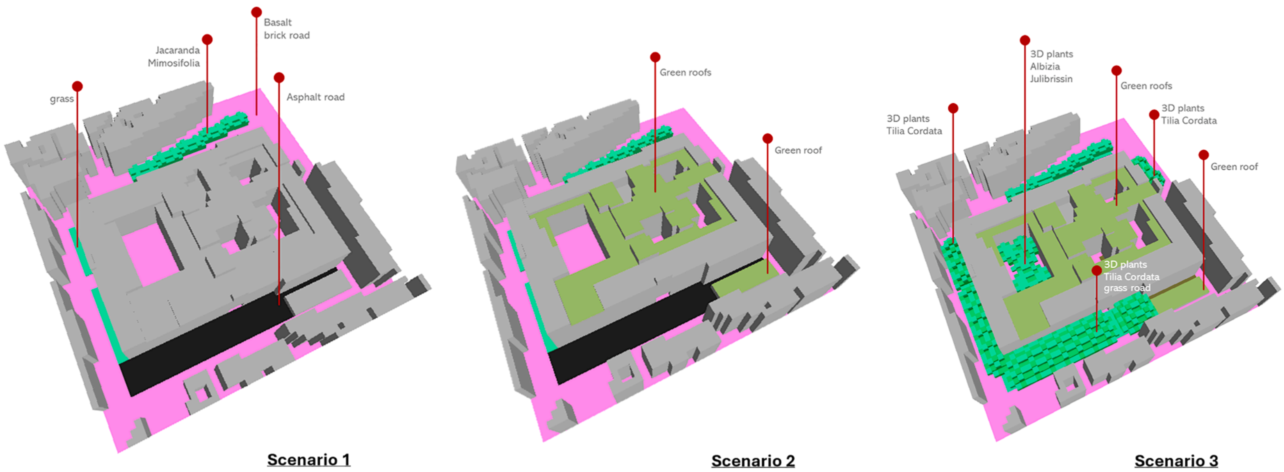

Fig. 3. Three intervention scenarios. Scenario 1: baseline; Scenario 2: green roofs on flat surfaces; Scenario 3: integrated greening strategies. Figures from Space (ENVI-met) reprocessed by the authors.

Table 2
Summary of existing and proposed greening interventions for each scenario.

Scenario	Green roof	Tree species	Number of trees	Pavements and draining surfaces
Scenario 1 – Baseline	None	Jacaranda mimosifolia	10	Basalt (roads, courtyards), asphalt (parking lot)
Scenario 2 – Design – only green roof	Extensive on flat asphalt surfaces; sandy loam substrate with air gaps	Jacaranda mimosifolia	10	Flat roofs replaced with extensive green roofs; historic pavements unchanged
Scenario 3 – Design -integrated green strategies	Extensive on flat asphalt surfaces; sandy loam substrate with air gaps	Tilia cordata, Albizia julibrissin Jacaranda mimosifolia	Tilia: main facade (10), parking (18), and small square behind (3) Albizia: internal courtyard (10) Jacaranda: (10)	Parking lot and square: grass-covered draining surfaces; internal courtyards: historic pavements unchanged with movable planters

Table 3
ENVI-met Input parameters settings.

STRATEGIES				
GREEN ROOF	**Substrate properties**		**Greening properties**	
	Emissivity	0.95	LAI	1.50
	Albedo	0.30	LAD	0.50
	Water coefficient	0.50		
TREE		**Jacaranda Mimosifolia**	**Tilia Cordata**	**Albizia Julibrissin**
	H (m)	15	20	12
	Width (m)	9	13	11
	Foliage shortwave albedo	0.60	0.18	0.60
	Foliage shortwave transmittance	0.30	0.30	0.30
	Emissivity of leaves	0.96	0.96	0.96
GRASS	H (cm)	25–50		
	Transmittance	0.30		
	Emissivity	0.97		
	Albedo	0.20		
SOIL SURFACE		**Basalt brick road**	**Sandy loam**	
	Volumetric heat capacity	2.386	0.435	
	Heat conductivity	1.73	34.1	
INDIVIDUAL PERSON SETTINGS	Age of person	35		
	Gender	Male		
	Height (m)	1.75		
	Weight (kg)	75		
	Body position	Standing		
	Walking speed (m/s)	1.20		
	Clothing insulation (clo)	0.5		

microclimatic comfort and the quality of open spaces. Circulation and parking surfaces are mostly made of basalt, a material with high thermal storage capacity; in addition, on the right side of the main entrance, there is a large asphalt-paved parking lot, which further intensifies heat absorption and subsequent re-radiation.

Vegetation is almost entirely absent: only ten *Jacaranda mimosifolia* trees, located to the left of the entrance (towards Via Carbonara), represent the sole arboreal element. However, they prove quantitatively and functionally insufficient to provide widespread shading and thermal mitigation. In front of the main entrance, neglected patches of lawn can be found, which fail to deliver significant ecological or microclimatic benefits. The inner courtyards, fully paved in basalt, share the same condition of impermeability and lack of vegetation.

From a building perspective, pitched roofs are made of clay tiles, while flat roofs are finished with bituminous membranes: both solutions, lacking green roof systems or high-reflectance surfaces, contribute to worsening the overall thermal balance of the site.

This initial overview therefore highlights the need to develop targeted climate adaptation strategies aimed at reducing heat accumulation, increasing permeability, and transforming the area into a healthier, more livable, and more resilient urban space.

2.2.2. Scenario 2: design – green roofs

Due to the high historical and architectural value of the Castel Capuano complex, located within a UNESCO World Heritage context, and the related conservation restrictions, it is not possible to implement invasive greening solutions. Installing green façades or radically altering the historic paving is not compatible with the preservation of the site;

therefore, such interventions were not considered. However, it is possible to introduce a series of targeted and non-invasive interventions aimed at improving the urban microclimate and reducing heat islands.

Within this framework, one of the most suitable and context-sensitive strategies concerns the implementation of green roofs on the flat portions of the building. As these internal surfaces are not visible from the ground level, particularly because they are obscured by parapets, such interventions neither alter the architectural profile nor compromise the historical value of the complex. Green roofs also provide significant benefits, such as improved thermal insulation, regulation of indoor temperatures, and contribution to stormwater management (Besir & Cuce, 2018; Castleton et al., 2010; Santamouris, 2014; Yang et al., 2023).

In Scenario 2, all the asphalt-covered flat roofs defined in Scenario 1 were replaced with an extensive green roof system (Cascone, 2019; Sommese, 2024) featuring an air gap and a sandy loam substrate. This configuration reduces summer overheating thanks to natural ventilation between the roof and vegetation, protects the waterproof membrane by preventing stagnation and moisture, and ensures a good balance between drainage and water retention for plant growth. The choice of extensive green roofs is primarily driven by the historical and architectural constraints of the Castel Capuano site. Extensive green roofs are less intrusive, impose lower structural loads, and minimize alterations to the original architectural features, making them more compatible with heritage protection requirements, structural integrity, and historical values.

As shown in the analysis of the results in Section 3, although green roofs represent an effective and context-compatible solution, they alone are not always sufficient to fully address the environmental and climatic challenges of the area. Hence the need to integrate additional widespread greening strategies, capable of extending the positive effects to the open spaces surrounding the complex.

2.2.3. Scenario 3: design – integrated greening strategies

In continuity with the previous scenario, the green roof interventions are complemented by additional greening strategies, calibrated to the potential of the context and the outdoor areas surrounding the complex. A first opportunity concerns the existing asphalt-paved parking area, whose redevelopment is planned through the use of natural permeable surfaces and the introduction of new tree plantings. The objective is to reduce soil impermeability, mitigate summer surface temperatures, and increase shading.

In the model for Scenario 3, the asphalt pavement of the parking area is replaced with permeable grass-covered surfaces, further integrated by the planting of *Tilia cordata*, a species characterized by a broad and dense, pyramidal or oval-shaped crown. This ensures consistent shading, contributes to the reduction of surface temperatures and to the mitigation of the UHI effect, and enhances air quality due to its capacity to capture atmospheric particulate matter (Moser et al., 2015; Pauleit et al., 2002; Rahman et al., 2017). The choice of linden (*Tilia cordata*) is particularly consistent with the historical sensitivity of the Castel Capuano context: while ensuring significant microclimatic benefits, it does not compromise the legibility of the architectural façade thanks to a balanced and easily manageable vegetative structure, and it harmonizes with the historical and landscape value of the site, enhancing its perceptual quality.

The green flowerbeds in front of the main façade of the building are further reinforced through the insertion of additional specimens of the same species (*Tilia cordata*), in order to amplify microclimatic benefits and consolidate vegetative coherence along the frontage.

Within the inner courtyard, without altering the historic paving, mobile and reversible solutions are proposed, such as large planters containing *Albizia julibrissin*. This species, owing to its wide yet light canopy, provides effective reduction of solar radiation and enhances the microclimatic comfort of the paved spaces. These characteristics, combined with its limited root impact and the ornamental value of its flowering, make it a particularly suitable choice for courtyards and historic spaces.

Finally, the rear square located on the north-east frontage, currently paved in basalt and characterized by the presence of the Formiello Fountain, could be redeveloped through the introduction of green elements and permeable grass-covered surfaces, capable of enhancing rainwater infiltration and reducing surface overheating. For this area, in fact, a limited substitution of part of the basalt paving with natural permeable surfaces has been envisaged, complemented by additional specimens of *Tilia Cordata*, thereby expanding shaded areas, fostering new opportunities for social interaction, and improving the overall comfort of the urban space.

2.3. Simulation settings and output results

The simulations were conducted over a 24-hour period, starting at 2:00 pm., taking as reference the hottest day of 2024 (11 August), identified based on air temperature records from the Naples Capodichino meteorological station, obtained from an online platform (Portale Meteo.it., 2024). Meteorological boundary conditions were defined based on the actual atmospheric recorded for that day, including air temperature, relative humidity, and wind speed (Table 4). The adopted values are representative of typical extreme but realistic summer conditions in Mediterranean climates and are consistent with the ranges reported in previous microclimatic ENVI-met studies conducted under comparable climatic contexts (Sommese et al., 2025; Sommese & Diana, 2025; Tousi et al., 2025).

It should be explicitly noted that no experimental validation of the simulated microclimatic outputs was performed, due to the lack of in-situ measurements for the specific case study area. Consequently, the simulations are intended as comparative scenario analyses rather than as fully validated quantitative predictions. In line with this limitation, the results are interpreted primarily in terms of relative differences, spatial–temporal trends, and physical plausibility, rather than the absolute magnitude of the simulated values.

For the evaluation of the microclimatic outputs generated by the ENVI-met model, five control points (P1–P5) were defined and distributed across representative positions of the case study (Fig. 4), corresponding to the main proposed interventions: main entrance (P1), main inner courtyard (P2), adjacent parking area (P3), rear square (P4), and street frontage (P5). The selection of these points was based on differences in solar exposure, the type of urban space, and the relationship with both built and permeable surfaces.

The extracted parameters were selected based on their relevance for the analysis of the UHI effect and pedestrian thermal comfort. Specifically:

- Potential Air Temperature (PAT, °C): a parameter reflecting perceived air temperature while accounting for atmospheric pressure, useful for spatial and temporal comparisons;
- Relative Humidity (RH, %): influences evaporation, transpiration processes, and thermal perception;
- Mean Radiant Temperature (MRT, °C): represents the weighted average of radiation exchanges from all surrounding surfaces,

Table 4
ENVI-met simulation settings.

General	
Start date (YYYY MM DD)	2024 08 11
Start time (HH:MM)	2:00 pm
Total Simulation time (h)	24
Meteorological data	
Tmax	37°C
Tmin	26°C
Tm	31°C
RH	40%

Fig. 4. Identification of control points (P1-P5): main entrance (P1), main internal courtyard (P2), adjacent car park (P3), small square behind (P4), road front (P5).

and is a key determinant of the radiant heat balance, indirectly providing information on the thermal comfort perceived by people;
- Wind Speed (WS, m/s): affects natural ventilation, heat dispersion, and convective cooling.

In addition to the analysis of the environmental microclimatic parameters, human thermal comfort indices were also evaluated, as they integrate the combined effects of air temperature, humidity, wind speed, and radiant conditions on the human body. Specifically:

- Universal Thermal Climate Index (UTCI, °C): evaluates outdoor thermal stress on the human body, providing a standardized assessment of heat and cold stress conditions;
- Physiological Equivalent Temperature (PET, °C): expressing the perceived thermal environment as an equivalent indoor air temperature under standardized conditions.

PET and UTCI are indices widely recognized and commonly applied in the scientific literature (Evgenia et al., 2024; Matzarakis et al., 1999; Pecelj et al., 2021) for the assessment of outdoor thermal comfort and thermal stress. They are based on the physiological responses of the human body, allow a comparative evaluation of comfort conditions under different simulated scenarios.

The simulations considered three design scenarios, generating a total of 60 combinations (3 scenarios × 4 parameters × 5 control points). All extractions were performed at a height of 1.40 m ($K = 3$), corresponding to the average pedestrian level, and commonly adopted in ENVI-met-based outdoor thermal comfort studies, in order to realistically represent human comfort conditions. It must be stressed that the input values for the wind speed analysis are based on the default data provided by the software, derived from nearby meteorological stations. While this approach does not capture specific on-site wind variability in detail, it is commonly adopted in ENVI-met studies at the neighborhood scale and is considered adequate for comparative scenario analyses. Accordingly, the analysis primarily focuses on the relative differences and spatial–temporal patterns among scenarios, rather than on the absolute magnitude of the simulated values, and the model outputs should therefore be interpreted as indicative of scenario performance rather than as exact site-specific quantitative predictions. To calculate the thermal comfort indices (PET and UTCI), the BioMet module of ENVI-met was used by adopting the default settings of the "standard human" model. Specifically, the reference individual corresponds to a 35-year-old male with default physiological parameters, as shown in Table 3. The only modification concerned the clothing insulation (clo), which was set to 0.5 instead of the default value of 0.90 clo, in order to reflect light summer clothing conditions consistent with the seasonal period of the simulations.

2.4. Data analysis and scenario comparison

The analysis of the results was conducted by integrating spatial evaluations, through output maps, and temporal assessments, through comparative graphs. This approach was designed to ensure a clear connection between the analyzed data, the specific study objectives, and the gaps identified in previous research.

Initially, output maps generated by Leonardo (ENVI-met) were processed, allowing the analysis of the spatial distribution of microclimatic parameters within the study domain. In particular, the following parameters were considered:

- Potential Air Temperature (PAT): to evaluate the cooling effect of the proposed greening interventions, addressing the need for quantitative assessments of temperature reduction in historic urban areas;
- Relative Humidity (RH): to assess localized increases associated with evapotranspiration processes, providing insight into microclimatic modifications linked to vegetation interventions;
- Mean Radiant Temperature (MRT): to identify areas of thermal stress and assess shading and cooling provided by green interventions, supporting objectives related to improve outdoor thermal comfort;
- Wind Speed (WS): to detect potential changes in ventilation patterns and heat dispersion, contributing to understanding the overall microclimatic impact of interventions.

Subsequently, numerical data were extracted at the five sampling points (P1–P5) for the four parameters (PAT, RH, MRT, WS) over a 24-hour period, to comparatively assess the simulated performance of individual and combined interventions in achieving the intended microclimatic improvements and enhanced thermal comfort. Comparative graphs were generated to show temporal trends across the three scenarios, allowing both the evaluation of individual interventions (Scenario 2) and the combined effects of integrated scenario (Scenario 3) relative to the baseline conditions (Scenario 1).

This integrated approach, based on spatial maps and temporal series, allowed the simultaneous analysis of both spatial and temporal dimensions of the phenomena, providing a comprehensive overview of the simulated impacts of greening scenarios on UHI mitigation and outdoor comfort. Subsequently, in order to further interpret and contextualize the obtained results, the output maps related to the human thermal comfort indices, UTCI and PET, generated by BioMet (ENVI-met), were analyzed both for the entire simulation domain and for each control point at 2:00 pm, which was identified as the time of maximum thermal stress during the day. UTCI and PET indices were considered to comparatively evaluate the simulated effects of the proposed greening strategies not only in terms of microclimatic improvements, but also with respect to the perceived thermal comfort experienced by humans within the modelled conditions.

3. Results

Fig. 5 presents the output maps generated by the Leonardo software for each of the four parameters analyzed across the three scenarios. The

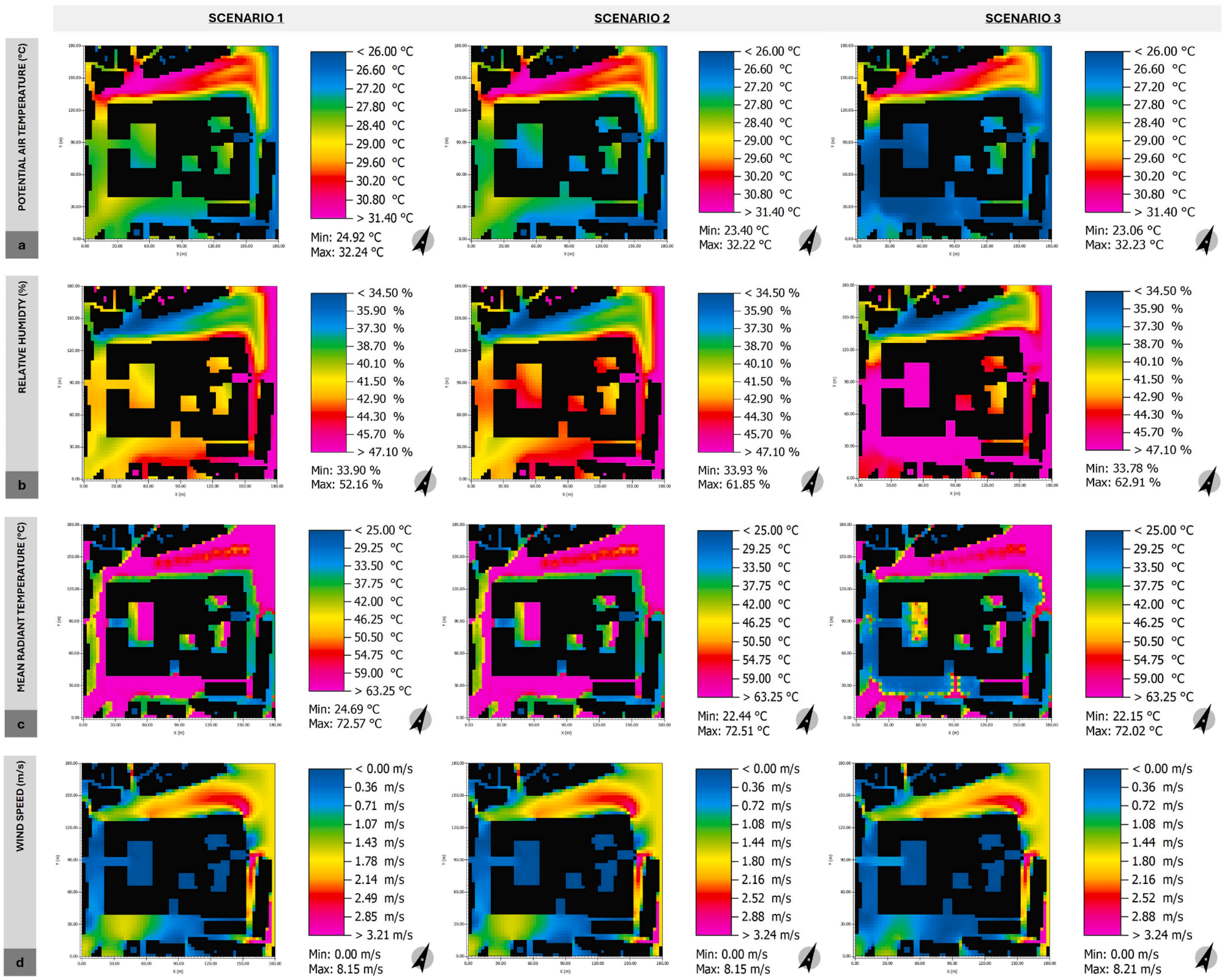

Fig. 5. Output simulations maps for the three scenarios (S1, S2, S3) with the four analyzed parameters (Potential Air Temperature, Relative Humidity, Mean Radiant Temperature, Wind Speed) at 2pm of 11th august. Figures from Leonardo (ENVI-met) reprocessed by the authors.

data shown in the maps refers to the values obtained at 2:00 pm, selected as the most affected.

In the baseline scenario, the potential air temperature (Fig. 5a) exhibits higher values, primarily concentrated in the north-eastern portion of the area and in some central zones, where color tones indicate widespread heat conditions. Areas with blue-green tones denote relatively lower values. With the introduction of green roofs (Scenario 2), these concentrations are attenuated, with a slight reduction in the intensity of the hottest zones. This cooling effect becomes more evident in Scenario 3, where cooler tones appear more uniformly and prominently distributed, particularly in areas affected by new tree planting, but also within the building complex. This spatial redistribution of cooler tones suggests a reduction in intensity and continuity of hot zones, indicating a broader and more diffuse thermal mitigation effect across the study area.

Regarding relative humidity (Fig. 5b), in Scenario 1 moderate values are observed, represented by dominant yellow-orange tones across most of the area, with limited spatial variability. Scenario 2 shows a shift towards red tones, especially along the south-east-west frontages and within the courtyards, reflecting localized increases in relative humidity due to green roof implementation. This effect is further amplified in Scenario 3, where red-magenta tones prevail, particularly along the south-east-west margins and in areas of tree planting and permeable surfaces. The result is a sharper gradient between compact built-up zones and open spaces, which appear significantly more humid.

The mean radiant temperature (Fig. 5c) in the baseline scenario highlights a critical situation: most of the area is dominated by magenta tones, indicative of strong surface heat accumulation typical of compact urban morphologies. Only marginal and open areas display cooler colors, though confined to limited extents. Scenario 2 produces only a partial and localized attenuation, with slight reductions in treated areas but without substantial modifications in the overall distribution. In contrast, Scenario 3 demonstrates the most significant change: the presence of trees and permeable surfaces introduces larger patches of blue and green tones, which disrupt the continuity of hot areas, especially along the margins and in open spaces, indicating widespread shading effects and reduced thermal accumulation in the most exposed zones. The pronounced MRT reductions in Scenario 3 are likely associated with the simulated effects of the implemented greening measures, including *Tilia Cordata* trees, permeable grass surfaces, and *Albizia Julibrissin* planters, which enhance shading and reduce radiative exposure during peak solar hours.

Finally, wind speed (Fig. 5d) in the Scenario 1 is very low, with dark blue tones dominating almost the entire area, interrupted only by narrow lighter bands along the edges and in slightly wider streets, reflecting limited ventilation permeability due to the compactness of the historic fabric. Scenario 2 shows an almost unchanged distribution, with only minor localized lightening near some treated roofs but without significant variations. In Scenario 3, however, the introduction of trees and permeable surfaces generates greater chromatic heterogeneity. Alongside darker areas, lighter zones emerge, suggesting that vegetation alters the simulated air flow patterns. For example, on the south façade, the presence of new trees reduces the wind speed, while under the tunnel of the main entrance, wind speed slightly increases, as suggested by the modelled pressure- and flow-regime redistribution within the internal courtyard.

3.1. Potential Air Temperature

In all control points (P1–P5), Scenario 1 consistently exhibits higher potential air temperatures compared to the other scenarios (Fig. 6). Scenario 2 shows a slight reduction relative to the Scenario 1, although the curves remain close. Scenario 3 displays the most pronounced effect: the green curve is generally lower, particularly during daytime hours, indicating a more consistent reduction over the full 24-hour period. Reductions are especially significant at P1 and P3, whereas at P4 and P5 the differences are more limited, suggesting that the effectiveness of the interventions depends on local position and morphology.

It is evident that the adoption of green roofs alone results in moderate reductions of potential air temperature, while their combination with additional greening interventions produces more substantial decreases, particularly during peak hours. These comparative trends suggest that integrated strategies are more effective in improving urban thermal comfort than isolated measures. The sole intervention with green roofs shows to have appreciable effects on internal courts. The following sections present a detailed analysis of the results for each control point.

3.1.1. Control point P1

Fig. 6a shows the hourly trend of potential air temperature at P1, following a typical diurnal cycle in all three scenarios, with minimum values in the early morning and maximum peaks between 13:00 and 14:00. Scenario 1 records temperatures ranging from 19.63°C to 28.03°C, Scenario 2 slightly lower (19.60–27.78°C), while Scenario 3 shows the lowest values, between 18.95°C and 25.99°C.

Delta analysis relative to the Scenario 1 (Fig. 6b) shows consistent but modest reductions In Scenario 2, with deltas ranging from 0.03°C to 0.26°C and an average daily decrease of approximately 0.10°C, with a stronger effect during afternoon hours and negligible impact at night. Scenario 3 generates significantly larger reductions, with deltas between 0.67°C and 2.03°C and a daily average decrease of about 1.18°C, with maximum values occurring during peak thermal hours, highlighting the stronger influence of the integrated scenario on daytime thermal conditions.

3.1.2. Control point P2

At P2, minimum temperatures occur in the early morning and maximum peaks between 13:00 and 14:00 (Fig. 6c). Scenario 1 ranges from 19.87°C to 27.64°C, Scenario 2 slightly lower (19.77–27.05°C), while Scenario 3 shows significantly lower values (19.36–25.93°C).

Compared to Scenario 1, Scenario 2 produces modest reductions in potential air temperature, ranging from 0.10°C to 0.63°C, with a daily average of about 0.28°C. Scenario 3 results in more pronounced reductions, between 0.50°C and 1.83°C, with a mean decrease of approximately 0.88°C (Fig. 6d). The greatest differences occur during afternoon peak hours, confirming the effectiveness of integrated strategies in reducing thermal load and enhancing microclimatic comfort.

3.1.3. Control point P3

Fig. 6(e) presents the hourly trend of potential air temperature at P3 for the three scenarios: minimum values in the early morning and maximum peaks between 13:00 and 14:00. Scenario 1 records 19.61–27.76°C, Scenario 2 slightly lower (19.59–27.60°C), while Scenario 3 shows significantly reduced values (18.99–25.98°C).

Delta analysis relative to the Scenario 1 (Fig. 6f) confirms that Scenario 2 produces very minor reductions (0.02–0.15°C, daily average ~0.06°C), whereas Scenario 3 achieves marked decreases between 0.59°C and 2.55°C, with a daily average of approximately 1.32°C.

3.1.4. Control point P4

The hourly trend at P4 also exhibits minimum values in the early morning and maximum peaks between 13:00 and 14:00 (Fig. 6g). Scenario 1 ranges from 17.93°C to 28.76°C, Scenario 2 shows nearly identical values (17.93–28.75°C), and Scenario 3 displays lower temperatures (17.93–27.15°C).

In terms of impacts and differences between scenarios (Fig. 6h), Scenario 2 does not result in significant reductions in potential air temperature, with deltas ranging from 0.00°C to 0.01°C and a daily average of approximately 0.01°C. Scenario 3, however, produces more substantial decreases, from 0.01°C to 1.86°C, with a daily mean of 0.63°C, the largest reductions occurring during peak afternoon hours.

3.1.5. Control point P5

As shown in Fig. 6i, the hourly temperature trend follows the diurnal cycle, with minima in the early morning and peaks between 13:00 and 14:00. Scenario 1 records 18.30–29.93°C, Scenario 2 (green roof) is almost identical (18.31–29.92°C), while Scenario 3 (green roof + integrated interventions) shows slightly lower values (18.09–29.56°C).

Fig. 6l highlights that Scenario 2 does not produce significant reductions in potential air temperature, with deltas near 0°C. Scenario 3 exhibits a more evident mitigating effect, with deltas ranging from −0.18°C to 0.89°C and a daily average of approximately 0.30°C, with maximum benefits occurring during afternoon peak hours.

3.2. Relative Humidity

The analysis of relative humidity across the three scenarios (Fig. 7) shows a similar diurnal pattern, with lower values during daytime and peaks between 04:00 and 06:00. Significant differences emerge in absolute terms: the integrated greening scenario (S3) shows the largest increase in relative humidity, especially at night and early morning, by up to 20 % compared to the Scenario 1. Green roofs alone (S2) show a generally limited impact on humidity levels, producing negligible changes compared to the Scenario 1 and only minor, localized, and marginal decreases at certain control points and times of day. In terms of comfort, it is important to note that an excessive increase in humidity in central hours of hot days may result in a sensation of discomfort.

3.2.1. Control point P1

At control point P1 (Fig. 7a), relative humidity is lowest in the early afternoon and gradually increases to peak in the early morning (around 04:00–05:00), before decreasing again toward the following afternoon. In Scenario 1, values range from 42.43% at 14:00 to 64.38% at 05:00. Scenario 2 follows a similar pattern with slightly higher values (min 43.26%, max 64.54%), while Scenario 3 shows more pronounced increases throughout the day (min 48.72%, max 67.52%).

The impact analysis relative to the Scenario 1 (Fig. 7b) indicates that Scenario 2 produces moderate and consistent increases in relative humidity, ranging from 0.21% to 1.91%, more noticeable in the afternoon and evening. Scenario 3 has a substantially larger effect, with increases between 4.57% and 12.90%, peaking in the afternoon and evening and remaining significant overnight, suggesting that the integrated interventions influence the daily humidity profile more markedly than the other scenarios.

3.2.2. Control point P2

At control point P2 (Fig. 7c), relative humidity exhibits a bell-shaped diurnal pattern across all three scenarios. In Scenario 1, values range from 42.54% at 14:00 to 63.16% at 05:00. Scenario 2 shows slightly higher values (min 44.57%, max 63.77%), indicating a consistent increase over the Scenario 1. Scenario 3 displays more pronounced increases, with minimum 48.46% and maximum 65.52%, reflecting the cumulative effect of the additional interventions.

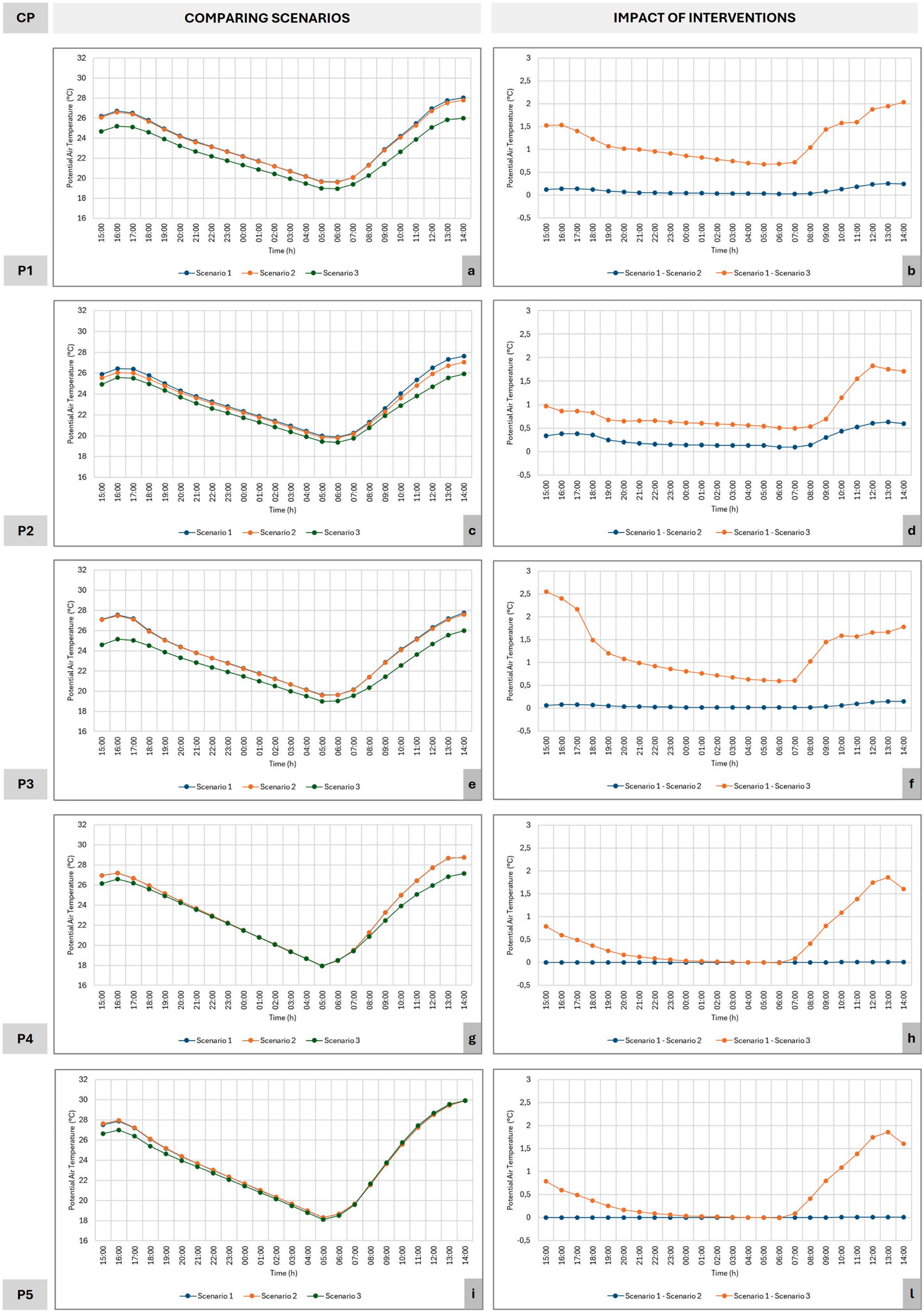

Fig. 6. Potential Air Temperature (°C). Scenario comparison: impacts of the interventions at the five control points (P1–P5).

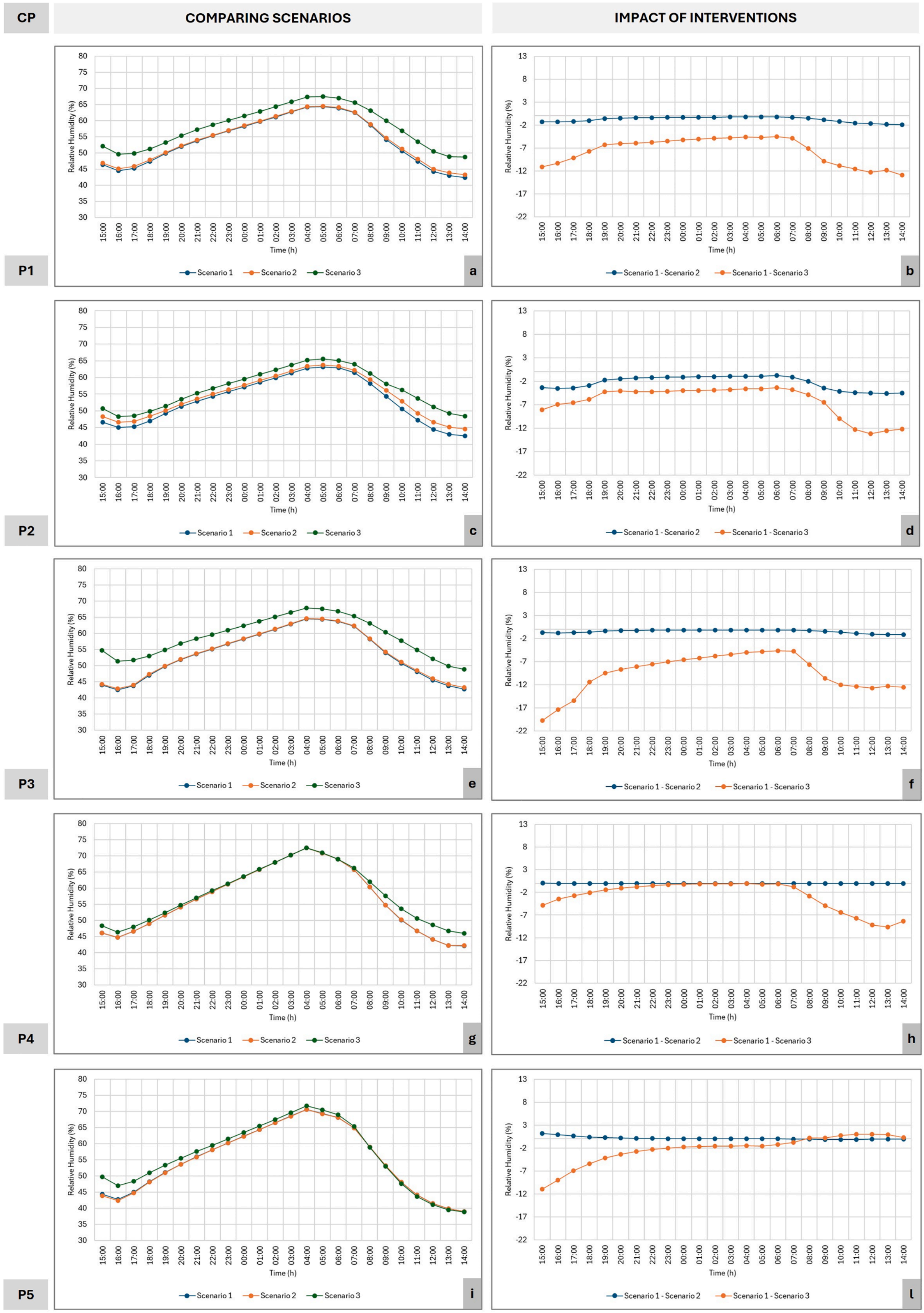

Fig. 7. Relative Humidity (%). Scenario comparison: impacts of the interventions at the five control points (P1–P5).

Impact analysis (Fig. 7d) reveals that differences between Scenario 1 and Scenario 2 range from −0.78% to −4.62%, more evident in the afternoon and morning hours. Differences between Scenario 1 and Scenario 3 are more substantial, oscillating between −3.35% and −13.20%, with peaks in midday hours. These results indicate a generalized increase in relative humidity under Scenarios 2 and 3, elevating both afternoon minima and nighttime peaks compared to the Scenario 1.

3.2.3. Control point P3

At control point P3 (Fig. 7e), relative humidity follows a typical bell-shaped diurnal pattern across all three scenarios. In Scenario 1, values range from 42.72% at 14:00 to 64.53% at 04:00. Scenario 2 shows slightly higher values (43.22–64.63%), while Scenario 3 exhibits a more pronounced increase, with minima of 48.87% and maxima of 67.92%, indicating that the additional interventions are associated with higher humidity levels compared to the Scenario 1.

Impact analysis (Fig. 7f) indicates that Scenario 2 induces modest changes relative to the Scenario 1with differences ranging from −0.14% to −1.16%, slightly more pronounced during midday. In contrast, differences between Scenario 1 and Scenario 3 are much larger, ranging from −4.76% to −19.73%, peaking in the afternoon, highlighting that the integrated measures in Scenario 3 produce a substantial overall increase in humidity throughout the day.

3.2.4. Control point P4

At control point P4 (Fig. 7g), relative humidity exhibits a clear daily progression across all three scenarios. In Scenario 1, values range from 42.18% at 14:00 to 72.48% at 04:00. Scenario 2 shows negligible increases relative to the Scenario 1(min 42.21%, max 72.49%), while Scenario 3 demonstrates more pronounced rises throughout the day (min 46.00%, max 72.53%), indicating a noticeable influence of the additional interventions.

Analysis of scenario differences (Fig. 7h) reveals that Scenario 2 has minimal impact compared to the Scenario 1, varying between 0.01% and −0.07%, showing near-complete overlap with Scenario 1. Scenario 3 produces more significant increases, with differences ranging from −0.07% to −9.59%, with the strongest effects in the afternoon and evening, indicating a generalized increase along the full daily curve. In summary, while Scenario 2 leaves relative humidity essentially unchanged, Scenario 3 results in a substantial elevation of both afternoon minima and nighttime peaks.

3.2.5. Control point P5

At control point P5 (Fig. 7i), relative humidity shows a typical diurnal cycle across the three scenarios. In Scenario 1, values range from 38.96% at 14:00 to 70.68% at 04:00. Scenario 2 exhibits slightly lower afternoon and evening values (min 38.98%, max 70.63%), indicating that the interventions in this scenario have minimal effect on humidity compared to Scenario 1. Scenario 3 shows more substantial increases, ranging from 38.85% to 71.77%, suggesting that the additional interventions elevate the entire relative humidity curve.

Impact analysis (Fig. 7l) indicates that Scenario 2 produces negligible changes relative to Scenario 1, ranging from a reduction of 1.19% to an increase of 0.02%, with slight decreases observed in the afternoon and evening. In contrast, Scenario 3 generates more pronounced differences, ranging from a reduction of 0.17% to an augmentation of 10.92%, with the largest increases in the afternoon and evening, while nighttime values stabilize around augmentation of 1.5-2%. These results indicate a consistent increase in relative humidity under the integrated scenario, whereas Scenario 2 produces almost no measurable impact.

3.3. Mean Radiant Temperature

Mean Radiant Temperature (MRT) is strongly influenced by solar radiation and surface conditions. Its absolute simulated values are sensitive to model assumptions, so the analysis focuses on relative differences and spatial–temporal patterns among scenarios to assess the comparative performance of the intervention. The analysis of MRT at the five control points (Fig. 8) compares the three intervention scenarios to evaluate the effectiveness of cooling strategies and identify the locations where the proposed measures produce the largest reductions in radiant temperature. As expected, the exclusive implementation of green roofs has no significant impact at the street level in terms of reducing mean radiant temperature.

3.3.1. Control point P1

Analysis of MRT at P1 (Fig. 8a) shows that Scenarios 1 and 2 exhibit very similar trends, with maximum values around midday and minimum values in the early morning. Peak MRT occurs around 13:00, reaching 63.53°C in Scenario 1 and 63.48°C in Scenario 2, while nighttime minima fall around 17–18°C between 04:00 and 06:00. Scenario 3, in contrast, presents a substantially lower profile, with daily peaks of approximately 30.46°C at 13:00 and nocturnal minima of 18.92°C at 02:00, indicating a pronounced reduction compared to Scenarios 1 and 2.

Impact analysis relative to the Scenario 1 (Fig. 8b) shows that Scenario 2 produces minimal differences, generally below 0.25°C, indicating a marginal effect on MRT. Scenario 3, however, shows large differences compared to Scenario 1, with differences exceeding 33°C during midday hours, suggesting a strong modification of the modelled radiative conditions associated with shading and surfaces changes. This marked contrast highlights the potential of integrated interventions to substantially reduce pedestrian radiant exposure during peak solar hours. The cooling effect is most pronounced during peak solar hours, while nighttime differences are smaller, with some hours showing Scenario 3 slightly warmer than the Scenario 1. This indicates that the interventions in Scenario 3 primarily act during periods of maximum thermal stress under the summer conditions.

3.3.2. Control point P2

At control point P2 (Fig. 8c), Scenarios 1 and 2 exhibit very similar MRT patterns, with maximum values concentrated during midday (approximately 60–61°C between 11:00 and 14:00) and minimum values during nighttime and early morning (∼18°C). Scenario 3, in contrast, shows a substantially lower profile throughout most of the day, with midday peaks around 58°C and similar nighttime minima (∼17–18°C).

Impact analysis relative to the Scenario 1 (Fig. 8d) indicates that Scenario 2 produces minimal differences, generally below 0.4°C, suggesting a negligible effect on MRT. Scenario 3, however, reduces MRT during peak hours, with differences up to 16°C around 14:00, indicating a relevant effect in limiting radiant heat load during the hottest periods. Nighttime and early morning differences are smaller, indicating that interventions in Scenario 3 are particularly effective in mitigating daytime heat and improving comfort during peak solar exposure.

3.3.3. Control point P3

At control point P3 (Fig. 8e), Scenarios 1 and 2 display very similar MRT patterns, with peak values during midday (approximately 63.3°C in Scenario 1 and 63.1°C in Scenario 2 between 11:00 and 14:00) and lower values at night and early morning (∼16–18°C). Scenario 3, in contrast, shows substantially lower peak temperatures, with midday maxima around 28°C, while nighttime minima remain comparable or slightly higher than in the other scenarios.

Impact analysis relative to the Scenario 1 (Fig. 8f) indicates that Scenario 2 produces negligible differences (<0.15°C), confirming minimal effect on MRT. Scenario 3, however, shows pronounced simulated reductions during peak solar hours, with differences exceeding 35°C around 14:00, indicating strong shading and surface modifications rather than a uniform air temperature decrease. The largest MRT reductions, similar to those observed at control point P1, coincide with areas directly shaded by the *Tilia Cordata* trees and the greening of the

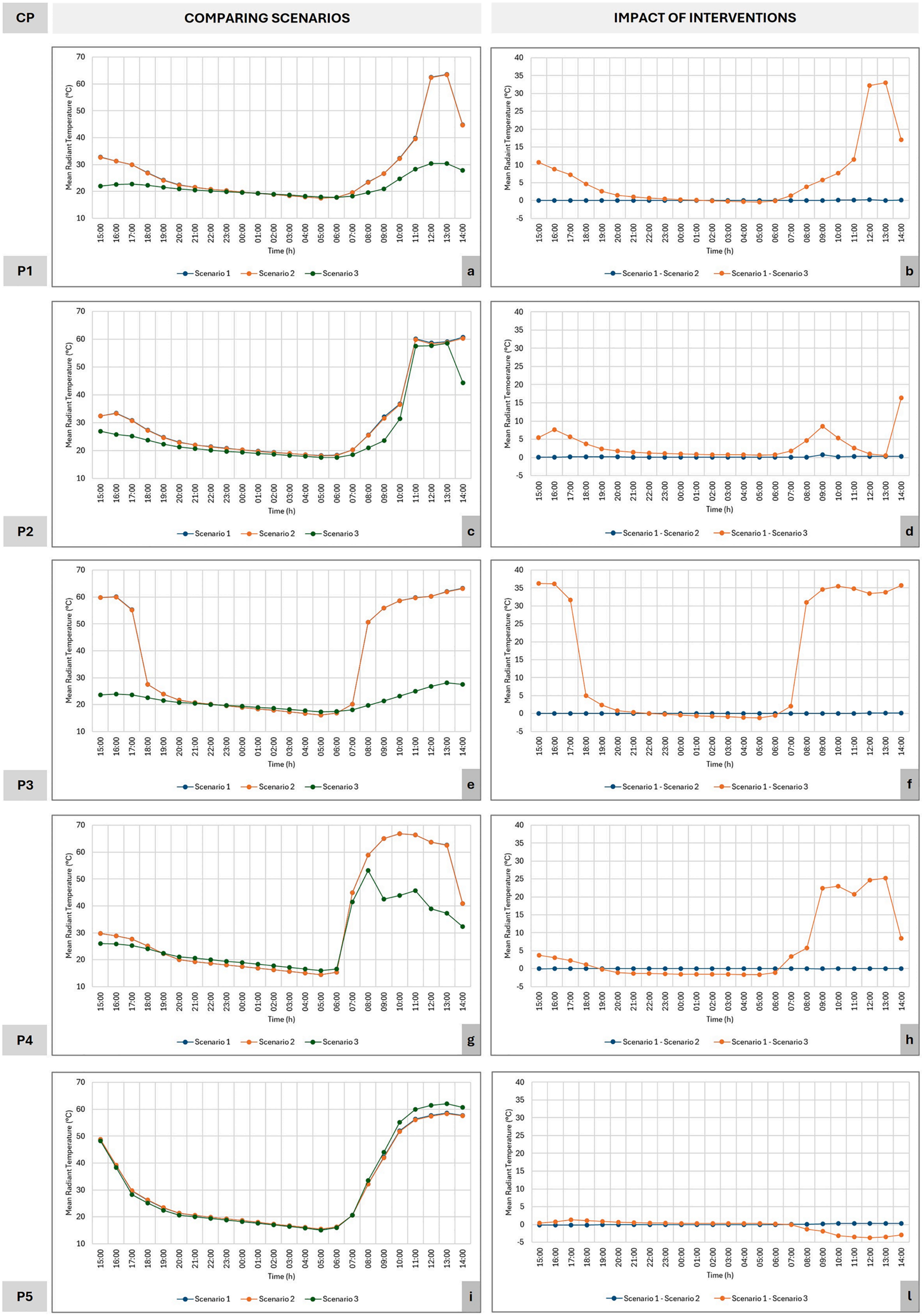

Fig. 8. Mean Radiant Temperature (°C). Scenario comparison: impacts of the interventions at the five control points (P1–P5).

asphalt surfaces, suggesting that the magnitude of change is driven by the combined effects of shading and surface cooling rather than model overestimation. Nighttime differences are smaller, and in some hours Scenario 3 may be slightly warmer, suggesting that the intervention is most effective during peak heat periods, enhancing thermal comfort at P3.

3.3.4. Control point P4

At control point P4 (Fig. 8g), MRT exhibits significant differences between scenarios, especially during midday. Scenarios 1 and 2 are nearly overlapping, with peak values between 09:00 and 11:00 exceeding 66°C and nighttime minima around 14–16°C, indicating that the intervention in Scenario 2 has a negligible effect on radiant temperature at P4. Scenario 3, however, shows a markedly different profile: midday temperatures are substantially lower (37–46°C), while nighttime values are slightly higher than in Scenarios 1 and 2 (16–18°C).

Impact analysis (Fig. 8h) confirms that differences between Scenario 1 and Scenario 2 are minimal (<0.01°C), whereas Scenario 3 produces substantial reductions during peak solar hours, with differences exceeding 25°C around 13:00 and over 23°C between 10:00 and 12:00. Nighttime differences are smaller, and Scenario 3 occasionally records slightly higher values. These results indicate that the interventions in Scenario 3 are primarily influential during peak heat periods, potentially improving radiant comfort at P4.

3.3.5. Control point P5

At control point P5 (Fig. 8i), mean radiant temperature (MRT) exhibits a daily cycle with nighttime minima between 15 and 16°C in the early morning (03:00–05:00) and daytime maxima around 58–59°C at midday (~13:00) for both Scenario 1 and Scenario 2, which show nearly overlapping profiles with negligible differences throughout the day. Scenario 3, however, stands out: nighttime values are comparable or slightly lower (15–17°C), while daytime peaks exceed 62°C between 11:00 and 13:00.

Impact analysis (Fig. 8l) confirms minimal differences between Scenario 1 and Scenario 2 (<0.35°C), indicating that the intervention in Scenario 2 does not significantly affect MRT at P5. Conversely, Scenario 3 produces a marked increase in MRT during midday, with differences reaching up to +3.7°C relative to the Scenario 1 between 11:00 and 13:00. Nighttime and early morning differences are smaller (0.3–0.8°C), occasionally favoring Scenario 3. This pattern indicates that the interventions in Scenario 3 at P5 have an adverse effect during peak solar radiation, contributing to an increased perceived thermal load.

3.4. Wind speed

At all control points, Scenario 2 shows negligible or slightly lower effects compared to the Scenario 1, indicating a minimal impact on wind speed trends at street level (Fig. 9). In contrast, Scenario 3 produces significant variations, with marked reductions at P1, P3, and P5, while at P2 and P4 it causes an increase, highlighting how the effectiveness of interventions strongly depends on local position and morphology. The observed reduction may be attributed to the presence of new trees blocking wind flow, while the increase may result from the presence of narrow passages that, through the Venturi effect, lead to higher wind speeds or create pressure differences that activate passive ventilation. Overall, Scenario 3 represents the most impactful simulation intervention on microclimate and urban ventilation.

3.4.1. Control point P1

The data show an increasing hourly trend in wind speed across all three scenarios (Fig. 9a), starting from approximately 0.33–0.34 m/s in the early afternoon and reaching peak values around midday of the following day. Scenario 1 exhibits a progressive increase from 0.334 m/s at 15:00 to a peak of 0.547 m/s around 11:00–12:00, followed by a slight decline. Scenario 2 follows a very similar pattern but with consistently slightly lower values, ranging from 0.328 m/s to a maximum of about 0.533 m/s. Scenario 3, however, stands out for significantly lower values throughout the observed period, increasing from 0.148 m/s to a maximum of around 0.245 m/s, showing a more subdued trend with less variability compared to the other two scenarios. In summary, the minimum values at the beginning of the period are 0.334 m/s, 0.328 m/s, and 0.148 m/s for scenarios 1, 2, and 3, respectively, while the maximum values reach approximately 0.547 m/s, 0.533 m/s, and 0.245 m/s.

Regarding the impact of the interventions (Fig. 9b), the comparison between Scenario 1 and Scenario 2 shows a consistent but minor reduction in wind speed, with differences ranging from 0.006 m/s to 0.015 m/s, indicating a slight but stable effect over the entire period. In contrast, the comparison between Scenario 1 and Scenario 3 reveals a much more pronounced reduction, ranging from 0.187 m/s to about 0.307 m/s during peak hours, indicating that interventions in Scenario 3 result in a substantial decrease in wind speed—up to twenty times greater than the differences between Scenario 2 and Scenario 1. Overall, Scenario 2 represents a moderate adjustment compared to the Scenario 1, while Scenario 3 entails a much more significant transformation, primarily due to the addition of new trees that may obstruct wind flow.

3.4.2. Control point P2

At control point P2, the wind speed dynamics differ from those observed at P1 (Fig. 9c). In Scenario 1, values start at approximately 0.129 m/s at 15:00 and gradually decrease to 0.105 m/s by 14:00 the following day, showing a slow declining trend throughout the period. Scenario 2 follows almost the same pattern, with nearly overlapping values, decreasing from 0.128 m/s to 0.106 m/s. In contrast, Scenario 3 consistently exhibits higher values, starting around 0.156 m/s and decreasing to 0.130 m/s, maintaining a level above the other two scenarios. The minimum values are 0.105 m/s, 0.106 m/s, and 0.130 m/s for scenarios 1, 2, and 3, respectively, while the maximum values at the start of the series are 0.129 m/s, 0.128 m/s, and 0.156 m/s.

Regarding impacts (Fig. 9d), Scenario 2 shows almost negligible differences compared to Scenario 1, ranging between +0.0005 m/s and −0.0005 m/s, indicating that the interventions have no significant effect on wind speed. By contrast, Scenario 3 exhibits a consistently negative difference of 0.021–0.027 m/s compared to Scenario 1, meaning that, unlike at P1, Scenario 3 here increases rather than decreases wind speed. This highlights that the impact of Scenario 3 interventions strongly depends on the control point: at P1, the intervention substantially reduces wind speed, whereas at P2 it tends to enhance it. This trend may be caused by the presence of new trees within an enclosed space, where the reduction of air pressure activates passive ventilation through the cluster's main gate to the outside.

3.4.3. Control point P3

At control point P3 (Fig. 9e), wind speed is significantly higher than at P1 and P2 and shows a steadily decreasing trend. In Scenario 1, values start around 1.79 m/s at 15:00 and gradually drop to about 1.26 m/s by 14:00 the following day. Scenario 2 follows almost the same pattern, with negligible differences from the Scenario 1, always below 0.0015 m/s. In contrast, Scenario 3 exhibits much lower values, decreasing from approximately 1.14 m/s to 0.66 m/s, maintaining a substantial gap throughout the period. Maximum values occur at the start—1.79 m/s for scenarios 1 and 2, 1.14 m/s for Scenario 3—while minimums at the end are 1.26 m/s, 1.26 m/s, and 0.66 m/s, respectively.

Regarding impacts (Fig. 9f), the difference between Scenario 1 and Scenario 2 is negligible, leaving the overall trend unchanged. Conversely, Scenario 3 shows a marked and consistent reduction in wind speed, with decreases exceeding 0.58 m/s and reaching 0.65 m/s during the early hours. Thus, at P3, Scenario 3 produces a strong and stable wind reduction, making it a much more impactful intervention compared to Scenario 2 and even stronger than at other control points.

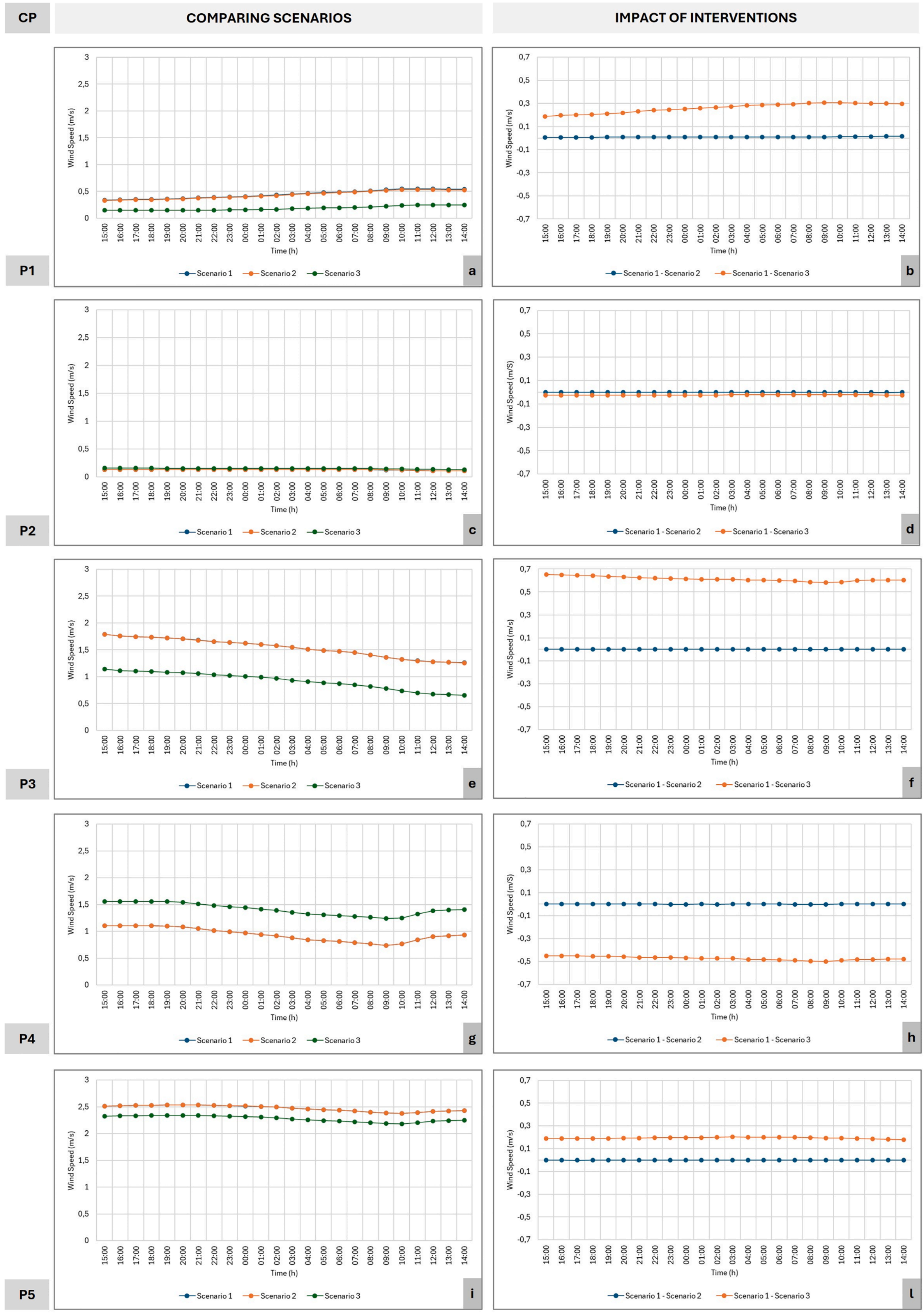

Fig. 9. Wind Speed (m/s). Scenario comparison: impacts of the interventions at the five control points (P1–P5).

3.4.4. Control point P4

The data at control point P4 indicate a clear diurnal pattern in wind speed across all three scenarios (Fig. 9g), with higher values in the afternoon and a gradual decrease during the evening and night, followed by a partial recovery toward late morning and early afternoon of the following day. In Scenario 1, wind speed starts at relatively high values around 1.11 m/s at 15:00, then progressively decreases to a minimum of approximately 0.74 m/s at 09:00, before increasing again to about 0.93 m/s at 14:00. Scenario 2 exhibits an almost identical temporal evolution, with wind-speed values consistently very close to those of Scenario 1 throughout the entire period, ranging from a maximum of about 1.11 m/s to a minimum of approximately 0.74 m/s. Scenario 3, by contrast, is always characterized by systematically higher wind-speed values. Values range from about 1.56 m/s in the afternoon (15:00–18:00) to a minimum of approximately 1.24 m/s around 09:00, followed by a gradual increase up to roughly 1.41 m/s at 14:00. Although the overall temporal trend is similar to that observed in Scenarios 1 and 2, Scenario 3 consistently exhibits wind speeds approximately 0.30–0.45 m/s higher than the Scenario 1.

Regarding impacts (Fig. 9h), the comparison between Scenario 1 and Scenario 2 confirms a negligible effect of the green roof alone on wind speed, with differences generally on the order of 0.001–0.002 m/s, well within numerical variability. In contrast, the comparison between Scenario 1 and Scenario 3 shows an increase in wind speed, ranging from approximately 0.50 m/s during the early morning hours to about 0.45 m/s in the afternoon. Overall, while Scenario 2 represents an almost neutral modification with respect to the Scenario 1, Scenario 3 leads to a significant alteration of the local wind field, more significant than in P2, suggesting that the combined intervention modifies airflow patterns more strongly than the green roof alone.

3.4.5. Control point P5

At control point P5 (Fig. 9i), wind speed shows a relatively stable trend with moderate absolute values. In Scenario 1, speeds start around 2.51 m/s at 15:00, decrease slightly to about 2.38 m/s by 10:00, and then rise slightly to 2.43 m/s in the afternoon. Scenario 2 follows a nearly identical pattern, with negligible differences (0–0.0014 m/s), indicating an almost null effect. Scenario 3 consistently exhibits lower values, with reductions between 0.18 m/s and 0.20 m/s, maintaining a stable gap throughout the period. Maximum values occur early in the series (≈2.53 m/s for Scenarios 1 and 2; 2.34 m/s for Scenario 3) and minimums range from 2.38 m/s to 2.19 m/s.

Regarding impacts (Fig. 9h), Scenario 2 shows a negligible, practically neutral effect, whereas Scenario 3 produces an appreciable reduction in wind speed (0.18 to 0.20 m/s), indicating a moderate but stable impact at this control point. In summary, while Scenario 2 barely alters wind dynamics, Scenario 3 achieves a clear and steady decrease, similar in nature and values to P1.

3.5. Human outdoor thermal comfort assessment via UTCI and PET

The spatial distribution of human outdoor thermal comfort, across the three simulated scenarios, at 2:00 pm (Fig. 10), corresponding to the period of maximum daytime thermal stress, highlights the strong dependency of human thermal stress on surface characteristics, vegetation structure, and radiative exchange within historically constrained urban environments. This result provides a comparative simulation-based model for evaluating the effectiveness of the proposed adaptation scenarios. The two parameters analyzed are: UTCI (Universal Thermal Climate Index) and PET (Physiological Equivalent Temperature).

Under Scenario 1, the study area exhibits severe thermal stress, with UTCI values exceeding 40°C across extensive portions of the site and PET peaks approaching 59°C. These values correspond to conditions of very strong to extreme heat stress, indicating a highly hostile microclimatic environment for outdoor human activities under the simulated extreme summer conditions. The spatial configuration of discomfort is closely associated with the dominance of dark, impermeable materials, namely basalt paving and asphalt surfaces, which exhibit high thermal inertia and low albedo, thereby amplifying heat storage. Notably, the courtyards, despite being partially shielded from direct solar exposure by surrounding building volumes, remain characterized by elevated UTCI and PET values. This suggest that, in dense historic fabrics, the absence of vegetation and the prevalence of mineral surfaces are associated with persistently high MRT, which appears to act as a dominant driver of thermal stress.

Considering the period of maximum daytime thermal stress (2 pm) all control points exhibit PET and UTCI values indicative of moderate to strong heat stress, with several locations reaching very strong thermal discomfort (Fig. 11). PET values range from 35.7°C (P4) to 49.1°C (P2), while UTCI values span between 31.2°C and 36.2°C. These results indicate that, the study area would be largely unsuitable for prolonged outdoor use. Points P2 and P3 emerge as the most critical locations, with

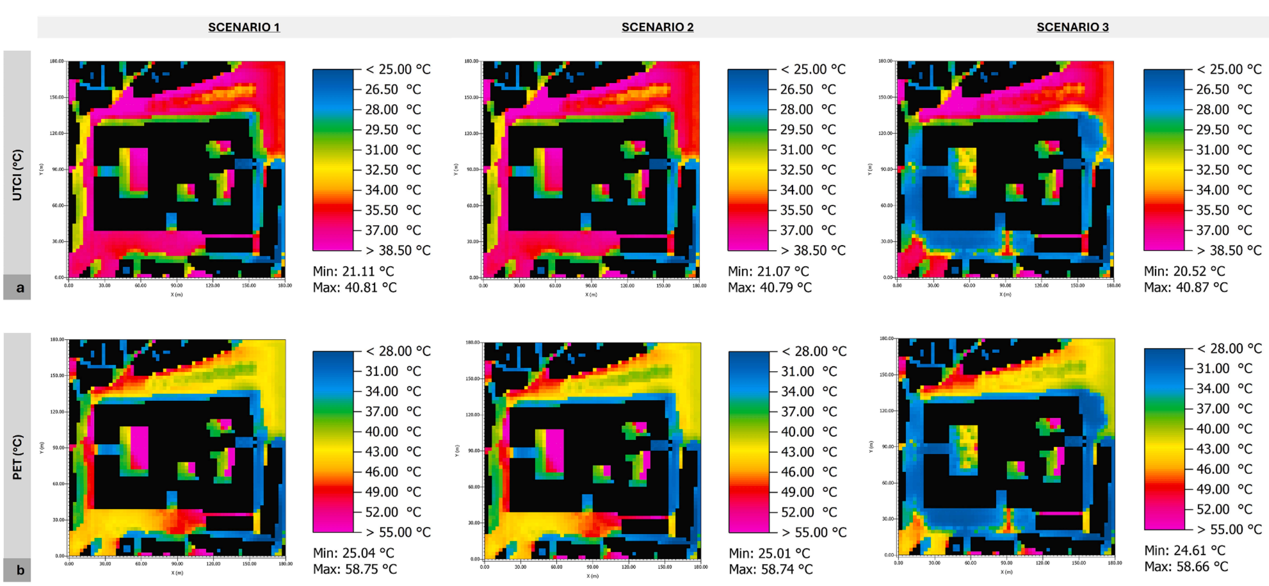

Fig. 10. Output simulations maps for the three scenarios (S1, S2, S3) with the two analyzed parameters (UTCI, PET) at 2pm of 11th august. Figures from Leonardo (ENVImet) reprocessed by the authors.

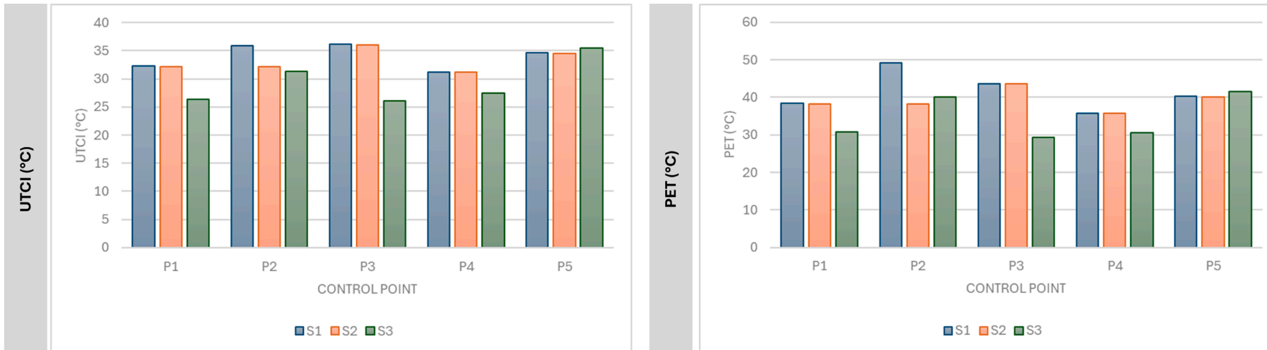

Fig. 11. UTCI and PET. Scenario comparison: impacts of the interventions at the five control points (P1–P5) at 2 pm time.

PET values exceeding 43°C and UTCI values above 35°C. This is likely associated with a combination of high MRT, direct solar exposure, and heat accumulation from mineral surfaces. Even relatively lower PET values at P4 highlight the lack of shading across the entire site.

The introduction of extensive green roofs (S 2) on flat roof surfaces produces a measurable yet limited attenuation of thermal stress. UTCI values show a modest reduction in average and peak values compared to the Scenario 1, indicating a partial mitigation of sensible heat fluxes to the surrounding air. However, the spatial distribution of PET remains largely unchanged, with maximum values still exceeding 58°C and extensive areas persisting in conditions of extreme thermal discomfort. This divergence between UTCI and PET responses is particularly instructive: while green roofs effectively reduce surface and indoor temperatures, their influence on pedestrian-level thermal comfort appears limited when not coupled with interventions affecting radiation at street level.

At 2 pm, across all points, reductions in PET and UTCI (Fig. 11) values between Scenario 1 and Scenario 2 are minimal, generally below 0.3°C, and in some cases practically negligible (P4 and P5). For instance, at P1, PET decreases by only 0.26°C (from 38.51°C to 38.25°C), while UTCI shows a similarly modest reduction of 0.23°C. Only at P2—one of the most thermally stressed locations—PET and UTCI show a substantial relative decrease compared to Scenario 1; however they still remain within strong heat stress conditions.

Scenario 3 shows the most substantial improvement in thermal comfort conditions. Both UTCI and PET maps reveal a pronounced reduction in peak values and a clear contraction of areas subjected to very strong and extreme heat stress. The emergence of cooler microclimatic zones corresponds closely with the introduction of permeable surfaces and tree canopies, suggesting a strong influence of vegetation and shading.. The impact is particularly evident in the PET distributions, which are highly sensitive to changes in MRT. Shaded areas beneath tree canopies exhibit markedly lower PET values, highlighting the effectiveness of arboreal shading in reducing radiant heat load a factor that cannot be compensated by roof-level interventions alone. The replacement of asphalt with grass-covered permeable surfaces further contributes to lowering surface temperatures and enhancing evaporative cooling, thereby reinforcing the cooling effect at pedestrian level.

The marked reduction and mitigation action induced by the interventions in S 3 is also confirmed by the point-in-time analysis at 2:00 pm. At points P1, P3, and P4, PET reductions between Scenario 1 and Scenario 3 range from approximately 5°C to over 14°C, shifting conditions from strong or very strong heat stress toward the lower bound of moderate stress. The most pronounced improvement is observed at P3, where PET decreases from 43.7°C to 29.4°C ($\Delta PET \approx -14.4$°C) and UTCI drops from 36.2°C to 26.1°C ($\Delta UTCI \approx -10.1$°C). This substantial simulated reduction suggests the key role of arboreal shading and surface permeability in lowering MRT and, consequently, perceived thermal stress. Similarly, P1 and P4 show consistent reductions in both indices, with UTCI decreases of approximately 6°C and PET decreases exceeding 5°C. Conversely, points P2 and P5 exhibit more moderate or inconsistent improvements. At P5, both PET and UTCI slightly increase in Scenario 3 relative to Scenario 1, suggesting residual exposure to solar radiation or insufficient canopy coverage.

4. Comparative analysis and discussion

The integrated analysis of the four microclimatic parameters highlights how the proposed interventions produce different simulated responses depending on the scale and combination applied. Green roofs (Scenario 2) appear largely marginal within the simulated scenarios, with benefits limited to slight increases in humidity (+1–2%) and minimal reductions in temperature or radiative load, confirming previous literature on the limited effectiveness of localized solutions (Oberndorfer et al., 2007). By contrast, the integrated scenario (Scenario 3), combining widespread greenery, tree planting, permeable surfaces, and green roofs, shows more pronounced and synergistic simulated impacts: MRT reductions exceeding 30°C, air temperature decreases of up to 2–3°C during peak thermal stress hours, relative humidity increases of up to 20%, and scenario-dependent modifications to local ventilation, with decreases in some areas and increases in others depending on morphology and spatial arrangement. This outcome aligns with recent studies emphasizing that tree shading and evapotranspiration are the most effective factors for improving summer comfort (Santamouris, 2014; Shashua-Bar et al., 2011), while introducing a comparative and site-specific quantitative perspective on the interaction of multiple concurrent interventions and their site-specific effect on urban ventilation. In this sense, the research suggests that only integrated and widespread strategies are more effective within the tested simulation model in UHI mitigation effects, surpassing the limited efficacy of single solutions, and provides a simulation-based basis to guide urban climate design toward systemic approaches.

4.1. Comparative analysis of environmental parameters at control points

The analysis of the environmental microclimatic parameter data summarized in the boxplots (Figs. 12–15) allows for a comparative assessment of the effectiveness of greening strategies across the three scenarios, in relation to the five control points distributed within the Castel Capuano area. Representing the data through statistical distributions provides more comprehensive information than simple averages or hourly peaks, highlighting the variability, range, and distribution of values for the four parameters analyzed.

For potential air temperature (Fig. 12), the Scenario 1 shows, for all the control points analyzed, the highest maximum value and, except for control point P1, the highest median value. Due to impermeable and thermally accumulative surfaces (asphalt, basalt), a strong variability of data can be seen, especially for control point P5 (from 18°C to 30°C). In the second scenario (green roofs) an appreciable reduction in median values is observed only at control point P2, while median values at the

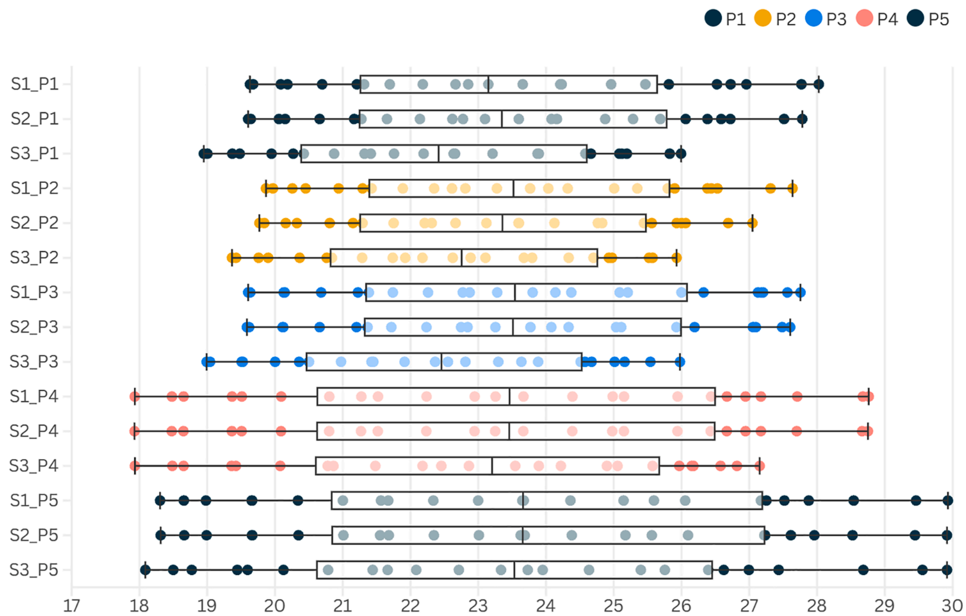

Fig. 12. Boxplot of air potential temperatures. The visualization shows, as indicated in the legend, each control point (P1-P5) for every scenario for every hour (S1, S2, S3).

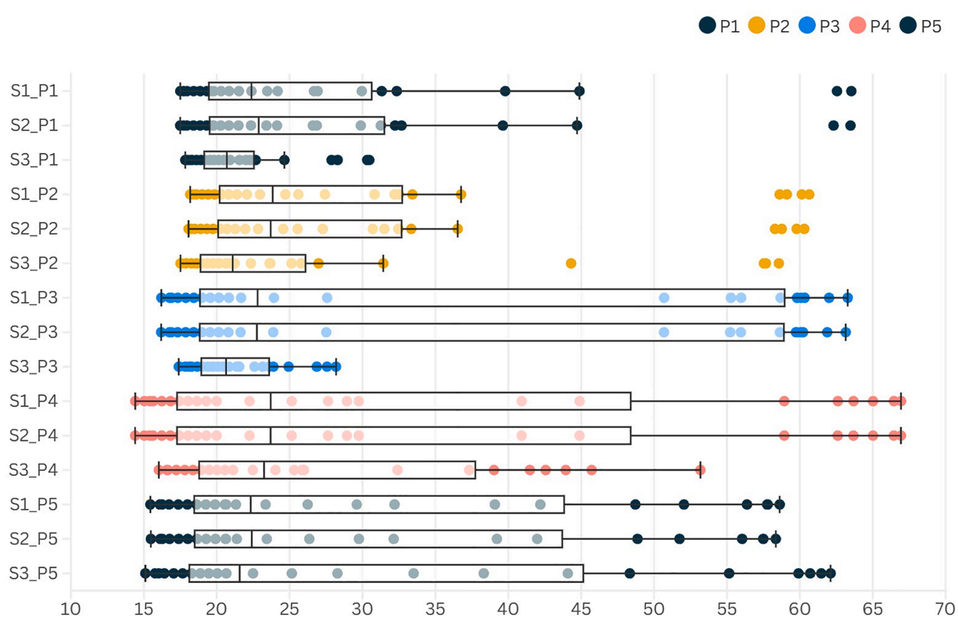

Fig. 13. Boxplot of mean radiant temperatures. The visualization shows, as indicated in the legend, each control point (P1-P5) for every scenario (S1, S2, S3).

remaining control points remain essentially unchanged. For P1, the median value of the distribution is even higher. In the green roof scenario, however, a notable reduction in maximum values is observed. At P2 in particular, this reduction exceeds 0.50°C. The fact that the most remarkable results produced by the green roofs are observed at control point P2 (inside the courtyard) confirms their effectiveness at the building scale, while indicating a limited impact on the surrounding urban microclimate, especially in dense historic contexts. Scenario 3, instead, shows more consistent simulated reductions. The median values of the distributions are lower than those of the Scenario 1 at all the control points, with reductions that for P1 and P3 arrive up to 1.0°C. The maximum value for P1 presents a reduction of 2°C compared to the Scenario 1. For P1, P2, and P3, the dispersion of data is reduced with greater thermal stability. The greatest benefits are observed in areas with targeted interventions (trees, permeable surfaces), while reductions are more modest in spaces less favorable due to morphology and orientation. Integrated strategies (Scenario 3) provide the most relevant benefits among the tested scenarios, particularly at points with higher solar exposure and where permeable surfaces have been introduced or replaced (P1, P3).

The variability of results across the control points highlights the importance of localized approaches tailored to the spatial and morphological characteristics of the area, rather than generalized solutions. These findings are consistent with international literature, which emphasizes the effectiveness of NbS when integrated into multifunctional systems distributed throughout the urban space (Norton et al., 2015). In particular, the combined adoption of green roofs, trees, and permeable surfaces is associated with reductions of surface and air

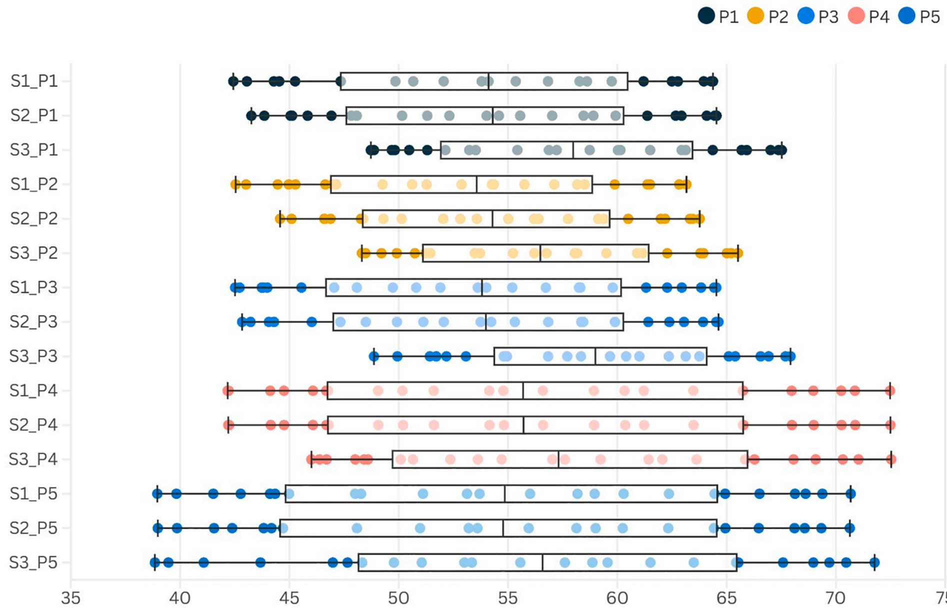

Fig. 14. Boxplot of relative humidity. The visualization shows, as indicated in the legend, each control point (P1-P5) for every scenario (S1, S2, S3).

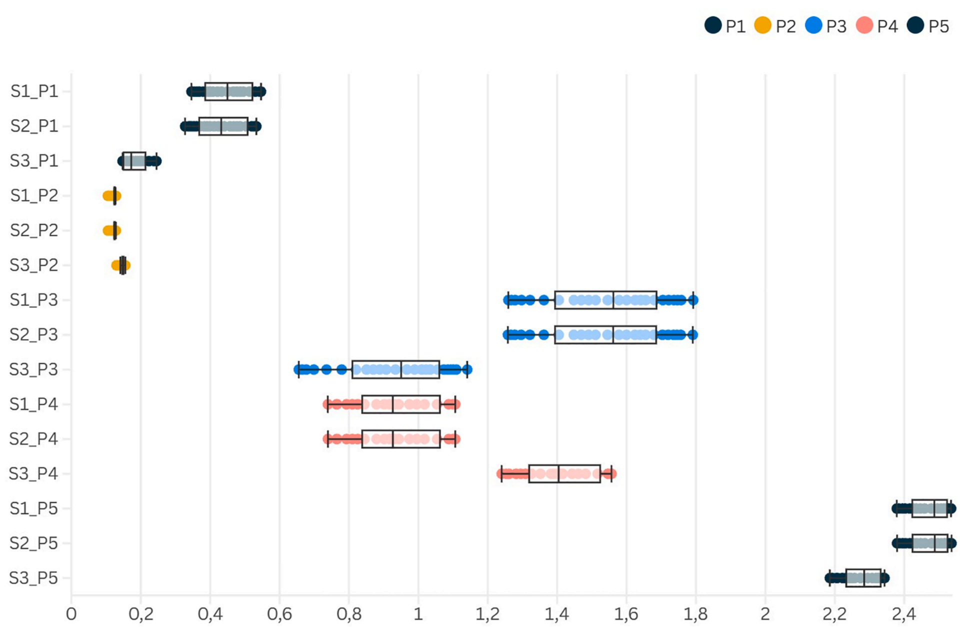

Fig. 15. Boxplot of wind speed. The visualization shows, as indicated in the legend, each control point (P1-P5) for every scenario (S1, S2, S3).

temperatures but also a mitigation of daily peaks and an improvement in the overall microclimatic resilience of the urban fabric (Gülten et al., 2016). This result indicates that, although green roofs are an effective measure in terms of building energy performance and help reduce thermal flows at the roof level, their direct effect on the surrounding urban microclimate remains limited in the high-density historic urban context.

Compared to PAT, MRT shows wider variations between scenarios and control points, reflecting the key role of surfaces and direct solar radiation in the pedestrian energy balance. The results are affected by the position of the considered control points since they are influenced by urban morphology and direct or indirect access to solar radiation. The analysis of Mean Radiant Temperature (Fig. 13) highlights how greening strategies differently affect radiative exchanges and thermal perception in outdoor spaces. Scenario 1, lacking vegetation and dominated by extensive mineral surfaces, exhibits stable medians for all control points (between 20 and 25°C) but peaks exceeding 65°C, with large variability especially at P3 and P4, indicating more critical microclimatic conditions. The adoption of green roofs (Scenario 2) marginally reduces the median values of MRT, except for P1, with differences under 0.5°C. This confirms their limited impact at the pedestrian level, with their main benefit being the reduction of PAT (Berardi et al., 2014). Concerning the whole distribution of data, also the boxes and the whiskers are in line with values of Scenario 1. Integrated strategies (Scenario 3), combining new trees and permeable surfaces, lead to more pronounced simulated MRT reductions, both in median and maximum values, especially at P1 and P3, and significant decreases at P2 and P4. Conversely, P5 shows a local increase (+2–4°C) likely due to radiant trapping effects, emphasizing the importance of site-specific design (Ghaffarianhoseini et al., 2015). In the case of Scenario 3, for P1, P2, and P3, a significant reduction in the variability of the distribution is shown. The distributions of the three scenarios for P1 and P2 exhibit outliers for higher values. Overall, the results indicate an improvement in radiant comfort compared to isolated measures, but their impact varies with urban morphology and solar exposure, requiring targeted calibrations to maximize benefits and minimize undesired effects.

For relative humidity (Fig. 14), Scenario 3 shows widespread increases compared to the Scenario 1 with medians rising from 53 to 55% (Scenario 1) to 57-59% considering all control points. For control points P1, P2, and P3, boxes and whiskers of Scenario 3 are significantly shifted towards higher values compared to Scenario1 while for P4 and P5 distributions are in line with Scenario 1 with a slight increase of lower thresholds of boxes (first quartile). Scenario 2 exhibits limited changes arriving up to 54-56% of median values but with distribution in line with Scenario 1, confirming a marginal impact of green roof-only interventions. The Scenario 1 scenario reflects a typical urban profile, with morning peaks above 65% and daytime lows around 40–42%, whereas green roofs (Scenario 2) produce only localized and negligible microclimatic effects. The integrated interventions of Scenario 3, combining trees and permeable surfaces, result in more compact distributions, with particularly pronounced increases in the afternoon and evening due to evapotranspiration. From the perspective of microclimatic comfort, these results confirm that integrated interventions based on a combination of vertical and horizontal vegetation, together with permeable surfaces, play a key role in restoring urban thermo-hygrometric balance. Such strategies not only reduce excessive radiant heating but also help mitigate the dryness typical of densely built urban spaces (Seo et al., 2023). At the same time, increases in relative humidity must be carefully considered in relation to overall thermal-hygrometric perception, since in already humid climates higher humidity may exacerbate the feeling of discomfort (Emmanuel & Loconsole, 2015).

The analysis of wind speed (Fig. 15) clearly highlights the influence of morphology and spatial configuration on the effects of mitigation interventions. The Scenario 1 shows marked variability across the five control points: P1 and P2 records low values, P3 and P4 intermediate, while P5 exhibits the maximum intensities of wind speeds. This dispersion reflects local heterogeneity, with exposed areas and others that are sheltered.

The introduction of green roofs (Scenario 2) does not significantly alter urban ventilation patterns: the boxplot distributions are almost identical to those of the Scenario 1, with mean differences below 0.01 m/s, confirming the negligible impact of localized interventions on wind speed.

Scenario 3, on the other hand, shows pronounced and site-specific effects, especially due to the addition of new trees. Wind speed is reduced at P1, P3, and P5, as indicated by lower medians, boxes, and whiskers compared to Scenario 1 and Scenario 2. At P3 the reduction exceeds 0.6 m/s for the median value. At P4, the wind speeds increase with the median value showing an increase of 0.50 m/s. In the court (P2), a slight local increase occurs: the formation of shade resulting from the newly planted trees and the presence of permeable surfaces and green roofs can facilitate micro-ventilation channels.

Overall, Scenario 3 emerges as the most effective simulated solution, showing site-specific changes in wind speed that may improve pedestrian comfort enhancing ventilation in previously stagnated zones. It is worth noting, however, that these improvements are accompanied by localized reductions in wind speed. Although the introduction of new trees locally reduces airflow, this drawback is minimal in a context where baseline wind conditions are already very low due to the compactness of the urban fabric. In this sense, the advantages provided by trees (e.g. shading, improved microclimatic quality) far outweigh the relatively negligible reduction in airflow at pedestrian level.

4.2. Discussions

The simulations highlight notable differences between single and integrated greening strategies. The scenario based solely on green roofs showed only marginal effects, with a PAT reduction of no more than 0.5°C and a relative humidity increase limited to just 1–2%. These limited results should be interpreted with caution. Previous studies indicate that the microclimatic performance of green roofs strongly depends on the extent of roof coverage (Jahangir et al., 2024; Knaus & Haase, 2020). When the percentage of vegetated roof area is relatively small, the resulting cooling and humidity-related effects may remain localized and are more effectively captured at the building scale (Krebs & Johansson, 2021; Schade et al., 2021) rather than at the neighborhood or pedestrian level. Thus, the modest impact observed in Scenario 2 reflects the limited roof coverage and the urban-scale assessment adopted, rather than an intrinsic inefficiency of green roofs. In the case study of Castel Capuano, microclimatic performance depends both on the size of vegetated areas and the characteristics of the building itself, which includes sloped portions unsuitable for green roof installation. Consequently, while certain benefits may occur at the building scale, the effect at the urban scale remains relatively limited; more substantial impacts would require the replication of similar interventions across multiple buildings to produce neighborhood-scale improvements. The effects at the pedestrian level attributable solely to green roofs are confined to the internal courtyard and remain extremely limited in extent and intensity. This condition is particularly relevant in the historic center of Naples, where several monumental buildings share typological and architectural characteristics with Castel Capuano.

In contrast, the integrated greening strategies scenario showed PAT decreases of 2–3°C, RH increases of up to 20–25 %, and reductions in surface MRT of up to 30°C, along with locally improved ventilation patterns under the simulated conditions.

Results are influenced by urban morphology and direct exposure to solar radiation and wind patterns. The various control points therefore exhibit heterogeneous results, with performance levels that vary depending on the specific conditions.

This is particularly evident in the case of the courtyard (P2), which exemplifies the hundreds of buildings with comparable conditions that characterize the historic center of Naples. In the courtyard, which is already partially shaded by the building itself, the potential air temperature shows slight decreases even with the simple green roof intervention (around −0.20°C in median value, and −0.60°C in maximum value). This measure is entirely non-invasive as green roofs are not visible from the ground level and remain respectful of the architectural value of the buildings. The addition of further shading in the court through the planting of new trees (Scenario 3) is associated with a reduction of MRT, reaching approximately −2.0°C in the median value and −5.0°C in maximum value. The comfort of the inner courtyard is further influenced by an increase in relative humidity and slight air flow. Considering these factors, Scenario 3 suggests an improvement in the courtyard's external comfort under the simulated conditions, transforming it into a pleasant space that can be considered as an extension of the surrounding public space, with non-negligible social impacts.

These results find partial confirmation in international literature but also extend its boundaries. The present study, while showing limited evidence of the benefits of green roofs, goes beyond the work of Ng et al. (Ng et al., 2012), who state that roof greening alone is ineffective for improving human thermal comfort at ground level, though it aligns with their findings on the greater effectiveness of trees in enhancing the outdoor microclimate. Urban tree-planting interventions, such as those described by Shashua-Bar (Shashua-Bar et al., 2011), have shown temperature reductions of 1–1.5°C, while combined approaches using greening and permeable materials achieve drops greater than 1–1.5°C, as also demonstrated by Chatterjee (Chatterjee et al., 2019) in Indian settings.In the present study, under the specific assumptions of the simulated extreme summer day and the selected urban configuration, the integrated scenario resulted in pronounced simulated reductions in simulated MRT, locally exceeding 30°C under peak daytime conditions. This values are higher than those typically reported in the literature for comparable greening measures; however, they should be interpreted as relative simulation-based differences driven by strong shading effects and reduced radiative exposure, rather than as exact quantitative predictions of real microclimatic conditions. The comparison is further limited by the single-day, model-based nature of the analysis. Similarly, the simulated increase in relative humidity, reaching 20–25%, exceeds the ranges commonly reported in previous studies (5-10%), and should therefore be interpreted cautiously as scenario-dependent responses under the adopted boundary conditions, suggesting a strong evaporative response induced by the combined application of tree planting, permeable surfaces, and green roofs within the specific boundary conditions considered in this study.

The originality of this research lies not only in its quantitative results but, above all, in its methodological approach. It represents a simulation-based application to a Mediterranean historic center subject to strict conservation constraints. The combined analysis of PAT, relative humidity, mean radiant temperature (MRT), and wind speed at five representative locations provides an integrated, multidimensional perspective rarely found in studies of dense historic urban contexts.

The analysis of results of parameters related to human thermal comfort indicates that integrated, pedestrian-scale greening strategies can potentially produce a substantial reduction in outdoor thermal stress during peak daytime conditions. In Scenario 3, UTCI values show simulated decreases of up to approximately 10°C (from ~36°C to ~26°C), while PET shows reductions exceeding 14°C in shaded areas, indicating a transition from very strong heat stress to conditions compatible with outdoor use. Such reductions are highly relevant from a public health perspective, as thermal stress mitigation of this magnitude is associated with a lower risk of heat-related morbidity, physiological strain, and cardiovascular stress, particularly among vulnerable population groups (Fong et al., 2018).

The comparison between UTCI and PET highlights the dominant role of MRT in shaping human thermal perception. PET proves more sensitive than UTCI to shading-induced reductions in MRT, confirming that interventions acting on radiative exchange—such as tree canopy shading and surface material modification—are critical for improving not only microclimatic conditions but also everyday urban livability. Enhanced thermal comfort supports pedestrian mobility, prolonged outdoor stay, and social interaction, thereby contributing to improved urban well-being.

The persistence of elevated thermal stress at locations characterized by discontinuous shading underscores the need for spatially precise and climate-responsive design. The coherence between the simulated MRT reductions and the corresponding changes in PET and UTCI supports the internal physical consistency of the modelled patterns, highlighting the dominant role of radiative shielding in outdoor thermal comfort under Mediterranean summer conditions, as produced by the integrated greening strategy of Scenario 3.

Beyond the microclimatic dimension, the proposed strategy has the potential to generate significant social value: lowering air temperature and MRT may help reduce health risks during heatwaves, particularly for the most vulnerable groups. The creation of shaded and comfortable spaces encourages daily use of public areas, promotes social interaction among residents, and strengthens neighborhood cohesion. Reversible, minimally invasive solutions also ensure compatibility with historic fabric, preserving cultural identity while enhancing the site's tourist appeal.

Overall, the findings suggest that systemic, multi-scale greening interventions are far more effective than isolated measures in mitigating the UHI effect and improving outdoor comfort in dense Mediterranean settings. NbS represent a key component of urban climate resilience, enabling historic urban areas to adapt to increasing heat stress while simultaneously promoting human health, comfort, and quality of life.

The results clearly demonstrate the greater effectiveness of integrated greening strategies compared to isolated interventions; however, they should be interpreted in light of several limitations related to the adopted design parameters, urban morphology, and modelling assumptions. The Castel Capuano case study is located in an extremely compact historic context, characterized by narrow streets, tall buildings, low sky view factors, and a pronounced lack of ground-level green spaces. These conditions significantly influence solar exposure, radiative exchanges, and ventilation regimes, thereby affecting the intensity and spatial distribution of the observed microclimatic effects.

It should be explicitly emphasized once again that no experimental validation of the ENVI-met outputs was performed due to the lack of in-situ microclimatic measurements for the specific case study area. Consequently, the results should be interpreted as simulation-based comparative trends rather than as fully validated quantitative predictions of actual site-specific conditions.

The selected design parameters, particularly the extent and placement of vegetated surfaces and the characteristics of tree canopies, directly influence the results. The limited effectiveness of the green-roof-only scenario is therefore attributable to the restricted availability of suitable roof areas and to typological and heritage-related constraints, rather than to an intrinsic inefficiency of the measure itself. Under these conditions, microclimatic benefits remain largely confined to the building scale and translate only marginally into improvements at pedestrian level, confirming the strongly site-specific nature of the findings. Furthermore, the adoption of extensive green roofs instead of intensive systems with deeper substrate layers, driven by the limited load-bearing capacity of existing structures, resulted in reduced achievable benefits.

4.2.1. Limitations and future research

This study adopts a scenario-based modelling approach to comparatively assess the microclimatic performance of various greening strategies in a complex historic urban context.

Although no in-situ experimental validation was conducted, the model setup was based on official meteorological data and widely adopted ENVI-met procedures. Consequently, the outcomes are interpreted in a comparative perspective, emphasizing spatial–temporal trends and relative differences among scenarios rather than exact absolute values.

Furthermore, the analysis refers to a single representative extreme summer day and to a highly compact historic morphology characterized by low sky view factors, enclosed courtyards, and limited ventilation permeability, which makes the results strongly site-specific and not directly transferable to other urban contexts without recalibration.

An additional consideration concerns the representation of vegetation, particularly tree canopies. While trees provide effective radiative shielding and contribute to the reduction of mean radiant temperature and thermal stress, they may also locally hinder airflow and modify ventilation patterns, especially in narrow urban canyons. This trade-off between shading benefits and potential reductions in air circulation is relevant in dense historic environments and suggests that integrated greening strategies should be carefully optimized to balance radiative cooling and ventilation.

Future research should include multi-day and seasonal simulations, field measurements for model validation, and more detailed parameterization of vegetation and local airflow to reduce uncertainty and improve the robustness and transferability of scenario-based microclimatic assessments in historic high-density urban areas.

5. Conclusions

This study evaluated the microclimatic effectiveness of various greening strategies applied in the Castel Capuano area, located in the historic center of Naples, where dense urban fabric, a lack of green spaces, and climate change-related challenges such as heatwaves are compromising the livability of the built environment and, consequently, the health and well-being of citizens. In conclusion, the main findings of the present study can be summarized as follows:

The scenario based exclusively on green roofs showed a positive but limited contribution to local microclimatic improvement, especially in the courtyard, with simulated PAT reductions not exceeding 0.5°C and RH increases limited to only 1–2%, highlighting that their isolated effect is not sufficient to significantly mitigate thermal stress conditions in public spaces of compact cities.

The combined approach of green roofs, shading, and street-level greening solutions shows the highest simulated microclimatic improvements among the tested scenarios, with local PAT reductions on the order of 2–3°C, increases in RH of up to 20–25%, and decreases in MRT of up to approximately 30°C, suggesting a potential improvement in outdoor thermal comfort under the modelled extreme summer conditions, particularly for the most vulnerable population groups.

Reductions in PAT and MRT are associated with an improvement in thermal comfort indices, with UTCI decreases of about 4–6°C and PET reductions of up to 8–10°C under the most critical conditions, often indicating a possible shift from strong/very strong heat stress classes to moderate stress levels.

The adoption of reversible and minimally invasive solutions suggests that heritage conservation can be reconciled with effective climate adaptation strategies, preserving the cultural identity of historic sites while simultaneously enhancing tourist attractiveness and the quality of public spaces, encouraging daily use and social cohesion.

Overall, this research provides simulation-based and context-specific guidance for planners, designers, and policymakers, indicating that carefully integrated, site-specific NbS can potentially reconcile microclimatic mitigation, architectural conservation, and social well-being, offering a methodologically replicable simulation model for climate-resilient regeneration of historic urban fabrics. This is especially true for large-scale historic buildings, swuch as Castel Capuano, where the architectural scale directly interfaces with the urban scale. These characteristics suggest that integrated interventions applied at the building level may generate relevant neighborhood-scale effects under comparable urban and climatic conditions.

CRediT authorship contribution statement

Francesco Sommese: Writing – review & editing, Writing – original draft, Visualization, Validation, Software, Methodology, Investigation, Formal analysis, Data curation, Conceptualization. **Lorenzo Diana:** Writing – review & editing, Supervision, Project administration, Funding acquisition.

Declaration of competing interest

The authors declare that they have no known competing financial interests or personal relationships that could have appeared to influence the work reported in this paper.

Funding

This research was funded by the European Union EU Next Generation Italian PRIN 2022 PNRR Programme under the “Greenwork—An interdisciplinary framework for urban health and urban resilience enhancement based on greening strategies on buildings and open spaces” project, CUP: E53D23019110001.

Data availability

No data was used for the research described in the article.

References

Alizadehtazi, B., Stolper, J., Singh, K., & Montalto, F. A. (2024). Microclimatic implications of a large-scale green roof and high-rise redevelopment in New York City. *Building and Environment, 250*, Article 111113. https://doi.org/10.1016/j.buildenv.2023.111113

IUCN. (2025). https://iucn.org/our-work/nature-based-solutions.

Portale Meteo.it.. (2025). Archivio Meteo Napoli Capodichino, 2024. https://www.ilmeteo.it/portale/archivio-meteo/Napoli+Capodichino/2024/Agosto.

Arnfield, A. J. (2026). Köppen climate classification. *Encyclopedia Britannica*. https://www.britannica.com/science/Koppen-climate-classification.

Aveta, A. (2022). Mutazioni e Prospettive d'uso: il caso di Castel Capuano. *Dall'Ingegneria militare all'architettura fortificata*. Napoli: Luciano Editore. Marina Fumo, Sommese Francesco (a cura di).

Berardi, U., GhaffarianHoseini, A., & GhaffarianHoseini, A. (2014). State-of-the-art analysis of the environmental benefits of green roofs. *Applied Energy, 115*, 411–428. https://doi.org/10.1016/j.apenergy.2013.10.047

Besir, A. B., & Cuce, E. (2018). Green roofs and facades: A comprehensive review. *Renewable and Sustainable Energy Reviews, 82*, 915–939. https://doi.org/10.1016/j.rser.2017.09.106

Brahimi, M., Benabbas, M., Altan, H., Nocera, F., & Costanzo, V. (2023). Enhancing urban microclimates: Potential benefits of greenery strategies in a semi-arid environment. *Sustainability, 15*(23), Article 16380. https://doi.org/10.3390/su152316380

Cafaro, R., Cardone, B., D'Ambrosio, V., Di Martino, F., & Miraglia, V. (2024). A new GIS-based framework to detect urban heat islands and its application on the city of Naples (Italy). *Land, 13*(8), 1253. https://doi.org/10.3390/land13081253

Cascone, S. (2019). Green roof design: State of the art on technology and materials. *Sustainability, 11*(11), 3020. https://doi.org/10.3390/su11113020

Castleton, H. F., Stovin, V., Beck, S. B. M., & Davison, J. B. (2010). Green roofs; Building energy savings and the potential for retrofit. *Energy and Buildings, 42*(10), 1582–1591. https://doi.org/10.1016/j.enbuild.2010.05.004

Chapman, S., Watson, J. E. M., Salazar, A., Thatcher, M., & McAlpine, C. A. (2017). The impact of urbanization and climate change on urban temperatures: A systematic review. *Landscape Ecology, 32*(10), 1921–1935. https://doi.org/10.1007/s10980-017-0561-4

Chatterjee, S., et al. (2019). Simulating micro-scale thermal interactions in different building environments for mitigating urban heat islands. *Science of The Total Environment, 663*, 610–631. https://doi.org/10.1016/j.scitotenv.2019.01.299

Chen, M., Li, X., Dang, A., Weng, Y., & Qiu, S. (2025). Adapting to heatwaves: Optimizing urban green spaces in Beijing to reduce heat health risks. *Sustainable Cities and Society, 130*, Article 106600. https://doi.org/10.1016/j.scs.2025.106600

Cohen-Shacham, E., Walters, G., Janzen, C., & Maginnis, S. (Eds.). (2016). *Nature-based solutions to address global societal challenges*. IUCN International Union for Conservation of Nature. https://doi.org/10.2305/IUCN.CH.2016.13.en.

Cuce, P. M., Cuce, E., & Santamouris, M. (2025). Towards sustainable and climate-resilient cities: Mitigating urban heat islands through green infrastructure. *Sustainability, 17*(3), 1303. https://doi.org/10.3390/su17031303

Diana, L., Sommese, F., Ausiello, G., & Polverino, F. (2024). New green spaces for urban areas: A resilient opportunity for urban health. In A. Cheshmehzangi, M. Sedrez, H. Zhao, T. Li, T. Heath, & A. Dawodu (Eds.), *Resilience vs pandemics: Innovations in public places and buildings* (pp. 37–53). Singapore: Springer Nature. https://doi.org/10.1007/978-981-99-8672-9_3.

Donthu, E. V. S. K. K., Long, Y. P., Wan, M. P., Zhou, M., & Ng, B. F. (2024). Dynamics of cool surface performance on urban microclimate: A full-scale experimental study in Singapore. *Sustainable Cities and Society, 102*, Article 105218. https://doi.org/10.1016/j.scs.2024.105218

Emmanuel, R., & Loconsole, A. (2015). Green infrastructure as an adaptation approach to tackling urban overheating in the Glasgow Clyde Valley Region, UK. *Landscape and Urban Planning, 138*, 71–86. https://doi.org/10.1016/j.landurbplan.2015.02.012

Evgenia, T., Mela, A., & Tseliou, A. (2024). Thermal stress in outdoor spaces during Mediterranean heatwaves: A PET and UTCI analysis of different demographics. *Urban Science, 8*(4), 193. https://doi.org/10.3390/urbansci8040193

Firozjaei, M. K., Kiavarz, M., Mijani, N., & Voogt, J. (2026). Ultra high-resolution mapping of urban surface temperature with multidimensional feature integration: A machine learning framework. *Advances in Space Research*. https://doi.org/10.1016/j.asr.2026.02.023

Fong, K. C., Hart, J. E., & James, P. (2018). A review of epidemiologic studies on greenness and health: Updated literature through 2017'. *Current Environmental Health Reports, 5*(1), 77–87. https://doi.org/10.1007/s40572-018-0179-y

Fortelli, A., Scafetta, N., & Mazzarella, A. (2016). Local warming in historical center of Naples: Urban heat island through thermic city analysis. *IJHT, 34*(S2), S569–S572. https://doi.org/10.18280/ijht.34S252

Frantzeskaki, N. (2019). Seven lessons for planning nature-based solutions in cities. *Environmental Science & Policy, 93*, 101–111. https://doi.org/10.1016/j.envsci.2018.12.033

Galanti, Giuseppe Maria, *Breve descrizione della città di Napoli e del suo contorno*. 1872.

Ghaffarianhoseini, A., Berardi, U., & Ghaffarianhoseini, A. (2015). Thermal performance characteristics of unshaded courtyards in hot and humid climates. *Building and Environment, 87*, 154–168. https://doi.org/10.1016/j.buildenv.2015.02.001

Gherri, B. (2023). The role of urban vegetation in counteracting overheating in different urban textures. *Land, 12*(12), 2100. https://doi.org/10.3390/land12122100

Gherri, B. (2024). Urban green spaces and their role in responding to the heat island effect in historical urban context. In J. R. Littlewood, L. Jain, & R. J. Howlett (Eds.), *Sustainability in Energy and Buildings 2023* (pp. 457–470). Singapore: Springer Nature. https://doi.org/10.1007/978-981-99-8501-2_40.

Grace, B., Bolleter, J., Barghchi, M., & Lund, J. (2025). Unpacking park cool island effects using remote-sensed, measured and modelled microclimatic data. *Land, 14*(8), 1686. https://doi.org/10.3390/land14081686

Gülten, A., Aksoy, U. T., & Öztop, H. F. (2016). Influence of trees on heat island potential in an urban canyon. *Sustainable Cities and Society, 26*, 407–418. https://doi.org/10.1016/j.scs.2016.04.006

Heshmat Mohajer, H. R., Ding, L., & Santamouris, M. (2022). Developing heat mitigation strategies in the urban environment of Sydney, Australia'. *Buildings, 12*(7), 903. https://doi.org/10.3390/buildings12070903

Jahangir, M. H., Zarfeshani, A., & Arast, M. (2024). Investigation of green roofs effects on reducing of the urban heat islands formation (The case of a municipal district of Tehran City, Iran). *Nature-Based Solutions, 5*, Article 100100. https://doi.org/10.1016/j.nbsj.2023.100100

Jamei, E., Thirunavukkarasu, G., Chau, H. W., Seyedmahmoudian, M., Stojcevski, A., & Mekhilef, S. (2023). Investigating the cooling effect of a green roof in Melbourne. *Building and Environment, 246*, Article 110965. https://doi.org/10.1016/j.buildenv.2023.110965

Knaus, M., & Haase, D. (2020). Green roof effects on daytime heat in a prefabricated residential neighbourhood in Berlin, Germany'. *Urban Forestry & Urban Greening, 53*, Article 126738. https://doi.org/10.1016/j.ufug.2020.126738

Kosanović, S., Marković, Đ., & Stamenković, M. (2025). New Belgrade's Thermal Mosaic: Investigating climate performance in urban heritage blocks beyond coverage ratios. *Atmosphere, 16*(8), 935. https://doi.org/10.3390/atmos16080935

Krebs, L. Fachinello, & Johansson, E. (2021). Influence of microclimate on the effect of green roofs in Southern Brazil – A study coupling outdoor and indoor thermal simulations. *Energy and Buildings, 241*, Article 110963. https://doi.org/10.1016/j.enbuild.2021.110963

Leonardi, S., Detommaso, M., Liotta, N. G., Distefano, N., Nocera, F., & Costanzo, V. (2025). Integrated strategies for air quality and thermal comfort improvement: The case study of the University Campus of Catania. *Applied Sciences, 15*(10), 5661. https://doi.org/10.3390/app15105661

Li, J., Zlatanova, S., & Stouffs, R. (2025). Cooling effects of urban green spaces: A systematic review of methods applied in the past two decades. *Sustainable Cities and Society, 133*, Article 106833. https://doi.org/10.1016/j.scs.2025.106833

Liu, Y., Bi, L., Hu, R., Ye, L., Zheng, W., & Lan, Y. (2025). Microclimate of outdoor tree-lined boulevards in university campuses in hot summer and cold winter regions: A case study of a University in Guilin. *Buildings, 15*(9), 1476. https://doi.org/10.3390/buildings15091476

B. Lopez, C. Kennedy, and T. McPhearson, 'Parks are critical urban infrastructure: Perception and use of urban green spaces in NYC during COVID-19', 2020, Preprints: 2020080620. doi: 10.20944/preprints202008.0620.v1.

Ma, X., et al. (2025). Evaluating the microclimatic performance of elevated open spaces for outdoor thermal comfort in cold climate zones. *Buildings, 15*(15), 2777. https://doi.org/10.3390/buildings15152777

Matzarakis, A., Mayer, H., & Iziomon, M. G. (1999). Applications of a universal thermal index: Physiological equivalent temperature. *International Journal of Biometeorology, 43*(2), 76–84. https://doi.org/10.1007/s004840050119

Moser, A., Rötzer, T., Pauleit, S., & Pretzsch, H. (2015). Structure and ecosystem services of small-leaved lime (*Tilia cordata* Mill.) and black locust (*Robinia pseudoacacia* L.) in urban environments. *Urban Forestry & Urban Greening, 14*(4), 1110–1121. https://doi.org/10.1016/j.ufug.2015.10.005

Naboni, E., Siani, R., Turrini, M., Touloupaki, E., Gherri, B., & Luca, F. D. (2023). Experiments on Microclimatically adapt a courtyard to climate change. *IOP Conference Series: Earth and Environmental Science, 1196*(1), Article 012032. https://doi.org/10.1088/1755-1315/1196/1/012032

Ng, E., Chen, L., Wang, Y., & Yuan, C. (2012). A study on the cooling effects of greening in a high-density city: An experience from Hong Kong. *Building and Environment, 47*, 256–271. https://doi.org/10.1016/j.buildenv.2011.07.014

Norton, B. A., Coutts, A. M., Livesley, S. J., Harris, R. J., Hunter, A. M., & Williams, N. S. G. (2015). Planning for cooler cities: A framework to prioritise green infrastructure to mitigate high temperatures in urban landscapes. *Landscape and Urban Planning, 134*, 127–138. https://doi.org/10.1016/j.landurbplan.2014.10.018

Nourian, M., Sanaieian, H., & Faizi, M. (2025). Enhancing urban heat island mitigation in region 12 Tehran: Integrating greenery and high albedo materials for improved thermal Comfort. *Energy and Buildings, 339*, Article 115724. https://doi.org/10.1016/j.enbuild.2025.115724

Oberndorfer, E., et al. (2007). Green roofs as urban ecosystems: Ecological structures, functions, and services. *Bioscience, 57*(10), 823–833. https://doi.org/10.1641/B571005

Pane, Roberto (1971). *Il centro antico di Napoli. Restauro urbanistico e piano di intervento, II*. Edizioni Scientifiche Italiane.

Pauleit, S., et al. (2002). Tree establishment practice in towns and cities – Results from a European survey. *Urban Forestry & Urban Greening, 1*(2), 83–96. https://doi.org/10.1078/1618-8667-00009

Pecelj, M., et al. (2021). Temporal analysis of urban-suburban PET, mPET and UTCI Indices in Belgrade (Serbia). *Atmosphere, 12*(7), 916. https://doi.org/10.3390/atmos12070916

Qin, H., & Zhou, B. (2025). Optimizing vegetation configurations for seasonal thermal comfort in campus courtyards: An ENVI-met study in hot summer and cold winter climates. *Plants, 14*(11), 1670. https://doi.org/10.3390/plants14111670

Rahman, M. A., Moser, A., Rötzer, T., & Pauleit, S. (2017). Within canopy temperature differences and cooling ability of *Tilia cordata* trees grown in urban conditions. *Building and Environment, 114*, 118–128. https://doi.org/10.1016/j.buildenv.2016.12.013

Romanello, M., et al. (2023). The 2023 report of the Lancet Countdown on health and climate change: the imperative for a health-centred response in a world facing irreversible harms. *The Lancet, 402*(10419), 2346–2394. https://doi.org/10.1016/S0140-6736(23)01859-7

Salata, F., Golasi, I., Petitti, D., de Lieto Vollaro, E., Coppi, M., & de Lieto Vollaro, A. (2017). Relating microclimate, human thermal comfort and health during heat waves: An analysis of heat island mitigation strategies through a case study in an urban outdoor environment. *Sustainable Cities and Society, 30*, 79–96. https://doi.org/10.1016/j.scs.2017.01.006

Salvati, A., Monti, P., Roura, H. Coch, & Cecere, C. (2019). Climatic performance of urban textures: Analysis tools for a Mediterranean urban context. *Energy and Buildings, 185*, 162–179. https://doi.org/10.1016/j.enbuild.2018.12.024

Santamouris, M. (2014). Cooling the cities – A review of reflective and green roof mitigation technologies to fight heat island and improve comfort in urban environments. *Solar Energy, 103*, 682–703. https://doi.org/10.1016/j.solener.2012.07.003

Schade, J., Lidelöw, S., & Lönnqvist, J. (2021). The thermal performance of a green roof on a highly insulated building in a sub-arctic climate. *Energy and Buildings, 241*, Article 110961. https://doi.org/10.1016/j.enbuild.2021.110961

Seidu, S., Chan, D. W. M., & Taiwo, R. (2025). Integrating green and grey infrastructure systems in dense urban regions: A synthesis of critical barriers and effective implementation guidelines. *Clean Techn Environ Policy, 27*(12), 7555–7576. https://doi.org/10.1007/s10098-025-03309-3

Seo, Y., Kwon, Y., Hwang, J. S., & Woo, D. K. (2023). A comparative experimental study of green roofs based on radiation budget and surface energy balance. *KSCE Journal of Civil Engineering, 27*(4), 1866–1880. https://doi.org/10.1007/s12205-023-1491-0

Shashua-Bar, L., Pearlmutter, D., & Erell, E. (2011). The influence of trees and grass on outdoor thermal comfort in a hot-arid environment. *International Journal of Climatology, 31*(10), 1498–1506. https://doi.org/10.1002/joc.2177

Smalls-Mantey, L., & Montalto, F. (2021). The seasonal microclimate trends of a large scale extensive green roof. *Building and Environment, 197*, Article 107792. https://doi.org/10.1016/j.buildenv.2021.107792

Sommese, F. (2024). Nature-based solutions to enhance urban resilience in the climate change and post-pandemic era: A taxonomy for the built environment. *Buildings, 14*(7), Article 7. https://doi.org/10.3390/buildings14072190

Sommese, F., & Diana, L. (2022). Il ruolo degli ospedali monumentali nelle strategie di adattamento al cambiamento climatico. *Urbanistica Informazioni*.

Sommese, F., & Diana, L. (2025). A holistic framework for the implementation of green roofs on existing buildings: A case study in the Mediterranean climate of Naples. *Building and Environment, 274*, Article 112811. https://doi.org/10.1016/j.buildenv.2025.112811

Sommese, F., Diana, L., Rezende da Costa, F., & Polverino, F. (2025). Effect of green roofs on external microclimate and runoff mitigation: Do they work in historical contexts? A case study in Naples. In R. Albatici, M. Dalprà, M. P. Gatti, G. Maracchini, & S. Torresin (Eds.), *Envisioning the Futures - Designing and Building for People and the Environment*. https://doi.org/10.1007/978-3-032-06974-0_34.

Tousi, E., Mela, A., & Tseliou, A. (2025). Nature-based urbanism for enhancing senior citizens' outdoor thermal comfort in high-density mediterranean cities: ENVI-met findings. *Urban Science, 9*(5), 152. https://doi.org/10.3390/urbansci9050152

Tsoka, S., Tsikaloudaki, A., & Theodosiou, T. (2018). Analyzing the ENVI-met microclimate model's performance and assessing cool materials and urban vegetation applications–A review. *Sustainable Cities and Society, 43*, 55–76. https://doi.org/10.1016/j.scs.2018.08.009

Xiong, N., et al. (2025). Simulation of microclimate and PM2.5 dispersion in typical urban parks in Beijing based on the ENVI-met model. *Sustainability, 17*(16), 7247. https://doi.org/10.3390/su17167247

Yan, D., Xu, L., Wang, Q., Feng, J., & Wu, X. (2025). Quantifying landscape effects on urban park thermal environments using ENVI-Met and 3D grid profile analysis. *Forests, 16*(7), 1085. https://doi.org/10.3390/f16071085

Yang, L., Li, X., Jareemit, D., & Liu, J. (2025). Vegetation configuration effects on microclimate and PM2.5 concentrations: A case study of high-rise residential complexes in Northern China. *Atmosphere, 16*(6), 672. https://doi.org/10.3390/atmos16060672

Yang, S., et al. (2023). Carbon dioxide reduction from an intensive green roof through carbon flux observations and energy consumption simulations. *Sustainable Cities and Society, 99*, Article 104913. https://doi.org/10.1016/j.scs.2023.104913

Zajacz, V. Takácsné, et al. (2025). Measuring local climate effects of institutional gardens in Budapest. *Land, 14*(9), 1768. https://doi.org/10.3390/land14091768

Zheng, X., et al. (2021). Outdoor thermal performance of green roofs across multiple time scales: A case study in subtropical China. *Sustainable Cities and Society, 70*, Article 102909. https://doi.org/10.1016/j.scs.2021.102909

Zuccaro, G., & Leone, M. F. (2021). Climate services to support disaster risk reduction and climate change adaptation in urban areas: The CLARITY project and the Napoli Case Study. *Frontiers in Environmental Science, 9*. https://doi.org/10.3389/fenvs.2021.693319